SNAKE: Harnessing Human Touch for Produce Quality Estimation to Foster Sustainable Retail Practices

ZHIGANG YIN, University of Tartu, Estonia
MARKO RADETA, University of Madeira, Portugal
MOHAN LIYANAGE, Fachhochschule Dortmund UASA, Germany
MAYOWA OLAPADE, University of Tartu, Estonia
ABDUL-RASHEED OTTUN, University of Tartu, Estonia
AGUSTIN ZUNIGA, University of Helsinki, Finland
PAN HUI, HKUST, Hong Kong and University of Helsinki, Finland
PETTERI NURMI, University of Helsinki, Finland
HUBER FLORES*, University of Tartu, Estonia

We present SNAKE, an innovative method that harnesses heat transferred from human touch interactions to estimate product quality. SNAKE offers an accessible and cost-effective solution that seamlessly integrates with existing retail practices; for example, it can be integrated with scales and cashiers already present in shops. Rigorous and systematic experiments demonstrate that SNAKE achieves a high level of accuracy (83%) and outperforms optical sensing and WiFi sensing baselines. We also provide evidence that SNAKE can capture touch interactions of different durations and maintain consistency across diverse user profiles and operating environments. To assess the potential for practical impact, we also carry out an additional user study (N=100) which suggests that SNAKE has potential to improve consumer purchasing decisions by at least 25% and reduce food waste (or increase promotional opportunities) by 10%-15%. In summary, our contribution offers a novel solution for leveraging smart IoT solutions to support retailing and foster sustainable retail practices.

CCS Concepts: • **Human-centered computing** → *Ubiquitous and mobile computing design and evaluation methods.*

Additional Key Words and Phrases: Thermal Sensing, Pervasive Computing, Internet of Things, Organic produce, End-user

ACM Reference Format:
Zhigang Yin, Marko Radeta, Mohan Liyanage, Mayowa Olapade, Abdul-Rasheed Ottun, Agustin Zuniga, Pan Hui, Petteri Nurmi, and Huber Flores. 2025. SNAKE: Harnessing Human Touch for Produce Quality Estimation to Foster Sustainable Retail Practices. 1, 1 (April 2025), 38 pages. https://doi.org/10.1145/nnnnnnn.nnnnnnn

*Corresponding author

Authors' addresses: Zhigang Yin, University of Tartu, Tartu, Estonia, zhigang.yin@ut.ee; Marko Radeta, University of Madeira, Madeira, Portugal, marko@wave-labs.org; Mohan Liyanage, Fachhochschule Dortmund UASA, Dortmund, Germany, mohan.liyanage@fh-dortmund.de; Mayowa Olapade, University of Tartu, Tartu, Estonia, mayowa.olapade@ut.ee; Abdul-Rasheed Ottun, University of Tartu, Tartu, Estonia, ottun@ut.ee; Agustin Zuniga, University of Helsinki, Helsinki, Finland, agustin.zuniga@helsinki.fi; Pan Hui, HKUST, Hong Kong and University of Helsinki, Helsinki, Finland, panhui@cse.ust.hk; Petteri Nurmi, University of Helsinki, Helsinki, Finland, petteri.nurmi@helsinki.fi; Huber Flores, University of Tartu, Tartu, Estonia, huber.flores@ut.ee.

XXXX-XXXX/2025/4-ART $15.00
https://doi.org/10.1145/nnnnnnn.nnnnnnn

1 INTRODUCTION

The sustainability of retail processes is a critical concern, with an estimated 17% of global food intended for consumption ending up as waste [64]. Organic produce with a limited shelf life is a major contributor of this waste [15] as they are often discarded due to decay or visual imperfections, such as color concerns, irregular size, or blemishes [62]. Consumers have a strong desire to reduce food waste but often lack the information that can drive the desired behaviors [25, 59]. Pervasive computing technologies have the potential to address this concern by offering insights into produce quality to reassure consumers to minimize unnecessary disposal. This not only benefits the consumers but can also aid retailers, e.g., by minimizing storage requirements and managing waste more efficiently.

Current solutions for produce quality estimation are difficult to deploy to retail environments as they lack the ability to seamlessly integrate with retail practices, often requiring specialized equipment or specific interactions. Instead, visual inspection by the naked eye remains the prevailing solution for both consumers and retailers [66]. While solutions for produce quality estimation exist, these primarily target other parts of the supply chain. Examples of relevant technologies include automated image processing [3, 44], wireless sensing [49], spectral imaging [39, 81] or optical (light) sensing [89]. With the exception of computer vision, all of these require specialized equipment and laborious interactions, making them unsuitable for consumers. Computer vision, in turn, only captures visual irregularities and thus effectively serves as a supplement to naked eye without being able to assure consumers on the actual quality of produce. Improving the situation requires accessible and cost-effective technical solutions that integrate with retail practices while concurrently provide informative and actionable information on reducing food waste and loss.

We contribute SNAKE, a pervasive sensing solution for produce quality estimation from natural human touch interactions. SNAKE improves on existing solutions by offering an accessible and low-cost solution that can seamlessly integrate with existing retail processes. As SNAKE harnesses natural interactions, it does not pose any interaction requirements on customers. The system is also cost-effective, only requiring a thermal camera (approx. \$500) or a thermal array sensor (\$10 − \$500 depending on resolution) to be installed at a location where it can monitor user interactions. SNAKE can also integrate with existing retail practices, e.g., as illustrated in Figure 1, the thermal camera can be integrated with scales making SNAKE able to estimate produce quality as part of existing practices. Households can also adopt SNAKE using a smartphone with a thermal camera or a USB-attached thermal camera.

SNAKE estimates produce quality by leveraging thermal radiation transferred from touch interactions. By monitoring the dissipation rate of this transferred heat, SNAKE extracts a dissipation fingerprint that characterizes the dynamics of thermal behaviour. Internal thermal characteristics of produce govern the rate at which the produce decays [10, 20], and these internal characteristics affect how the produce exterior absorbs and reflects thermal radiation. The dissipation fingerprint extracted by SNAKE captures these changes in thermal behavior, and uses them to estimate produce quality. However, accurately estimating thermal characteristics from opportunistic human touch interactions is highly challenging as surface variations, distinct interaction patterns, and the ambient environment affect thermal transfer. Different produce types exhibit unique thermal properties that affect heat dissipation rates and external temperature fluctuations (e.g., refrigerated vs. room environments) further complicate modeling. SNAKE overcomes these challenges by leveraging an innovative modeling pipeline that compensates against these variations, ensuring consistent and accurate produce quality estimation across diverse user interactions and ambient conditions. Specifically, SNAKE uses computer vision techniques to accommodate variations in human touch patterns, including the size of the touched region and the duration of the interaction. Additionally, compensation models are integrated to account for variability in hand temperature and the ambient temperature.

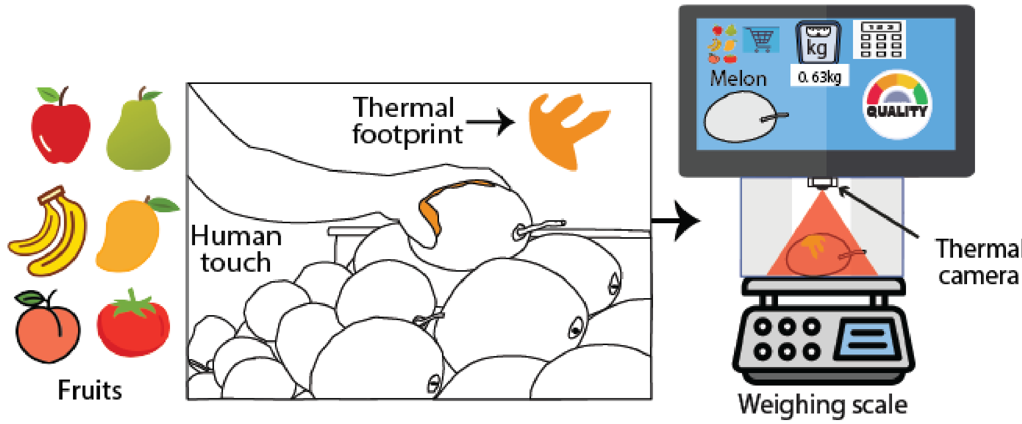

Fig. 1. SNAKE Produce Quality Estimation.

Systematic and rigorous independent evaluations conducted over time, involving multiple users, the five most prominent produce categories, and diverse interaction patterns, demonstrate that SNAKE achieves approximately 83% accuracy in estimating produce quality and outperforms state-of-the-art baselines, including optical and WiFi sensing. Independent studies conducted over repeated intervals with the same produce type validate our methods. Our evaluation demonstrates that thermal radiation induced by touch interactions is sufficient for capturing produce decomposition and that thermal dissipation values closely relate to firmness values, validating the theoretical model underpinning our approach. We also demonstrate that SNAKE can operate robustly across different ambient environments, individuals touching the produce, and touch duration patterns. We also conduct smaller-scale experiments with additional produce and conditions to demonstrate that SNAKE can be generalized to a wider range of produce and that it can operate effectively in the long term. Finally, we evaluate the practical potential of SNAKE through a user study with 100 participants that compares our method to traditional manual inspection. We developed a prototype integrating SNAKE with standard retail scale appliances. The prototype uses a 3D-printed deployment designed to simulate real-world retail scenarios. User evaluations of this new prototype solution indicate that SNAKE can enhance consumer purchasing decisions by at least 25% and reduce food waste by 10% to 15%, demonstrating significant economic benefits that warrant its adoption in retail environments. Additionally, we provide an in-depth discussion on the integration and implementation of SNAKE, addressing potential challenges for user perception and emphasizing the minimal barriers to its deployment in real-world retail settings. Taken together, our work offers a promising, effective, and innovative solution for supporting produce quality estimation by harnessing human interaction patterns.

2 RELATED WORK

Produce quality monitoring: Manual inspection is the most common method for produce quality estimation. While easy to implement, it is highly laborious, prone to errors, not scalable, and very inefficient [88]. Automated systems have been developed to overcome these limitations and are mostly powered by computer vision [7]. These methods, however, are sensitive to illumination and occlusions and high-quality footage, requiring an unobstructed view of the produce's surface to be able to estimate quality. Some CV-based applications are already available on app stores to evaluate produce quality (e.g., Clarifruit and Intello Track). These apps are mainly for businesses instead of small retailers and customers. They require ongoing subscription fees, and the cost is unlimited. Besides the image quality, user factors can also affect the final results in the apps, as they need to fill up the defect. This undoubtedly requires user expertise with extra burden. In addition, Clarifruit requires the Brix values (sugar content) of produce, which can be measured by refractometer and spectrometer. However, the refractometer is destructive and can cause produce waste. The spectrometer is non-destructive but very expensive (e.g., F-750 produce quality meter around 10000 dollars). Intello Track app has region limitations at present and users in a few countries (USA, Singapore, and India) can register.

The main alternative to visual techniques is spectral imaging, such as near-infrared (NIR) sensing [39], hyperspectral imaging [24, 81], or specific light wavelength imaging [60, 89], depending on the parts of the light spectrum considered. Although these methods capture additional details about produce, they require costly, bulky, and specialized equipment, making them impractical for end-users. For example, NIR sensing is used in commercial spectrometers for non-destructive internal fruit measurements, but deploying this technology at scale is expensive. Wireless signals can also estimate the water content of the produce [36]. However, these techniques are highly sensitive to the measurement setup and dynamic environment and can only measure one item at a time. High-quality cameras are also needed to improve the accuracy of moisture and soluble solids content measurements in wireless sensing [49]. Similarly, thermal imaging has been explored in agriculture for applications such as harvesting and manufacturing [2, 16, 53, 78]. Thermal imaging typically detects bruises or diseases in produce on the basis of surface temperature. However, this analysis is not tailored to user perception or interactions. We advanced thermal imaging by developing a user-friendly solCution that assists humans in estimating produce quality in practical deployments.

Customer-center solutions: Customer-oriented solutions have been developed using smart IoT and wearable devices for end-users to assist their daily activities. For instance, users can take pictures of their food using their mobile camera to analyze calorie intake [63]. Cameras attached to the inside of a refrigerator door can monitor food inventory, plan shopping, and reduce household waste [22]. Some mobile applications are developed to reduce food waste, e.g., improving fridge storage practices [50], bridging the gap between waste instances and past user-behavior reflection [23, 86]. A smartfridge network utilizes IoT devices such as particle photons and a companion app for remote browsing and reservation of food donations, improving food distribution and addressing food insecurity [4]. Tools for online food shopping websites and in-store interactive displays or tablets are used to support sustainable food shopping for stakeholders by providing eco-feedback visualizations and guidance on environmentally friendly products [48, 70, 72]. Other IoT devices (e.g., TV) are also used to minimize food waste, e.g., user education and awareness promotion by interactive gameplay [73]. Likewise, RFID stickers have been used to learn the quality of food via wireless [30]. Other sensors can also be utilized to support better decision making [28], for instance, when buying groceries at a shop and disposing or preserving household produce [38]. The wearable FitNibble utilizes a proximity sensor and IMU to monitor hand-to-mouth gestures and chewing, addressing challenges in automating food journaling for better dietary habits [5]. Other wearables can also be placed in different body positions (wrists, ear and neck) to monitor food intake for health suggestions by various sensors (piezoelectric, acoustic or EMG/ EGG) [33]. Other work has investigated the miniaturization and portability of spectral technologies, such that it is possible to integrate into handheld devices [85] and smartphones [14]. Unlike others, we rely on COTS thermal cameras to provide end sales solutions that support the customers through natural human touch interactions. SNAKE can be deployed in any personal (smartphone [17]), wearable (smart ring [87]) or user-assisted (scanner [45]) device.

Smart retail solutions: Smart IoT (Internet of Things) devices are enhancing retail activities and optimizing retail experiences [79]. An intelligent mobile grocery assistant is developed to support customers during grocery shopping by creating shopping lists and providing personalization [9]. Other smart applications provide information on products (e.g., expiry date, quality indicators and offers) to understand consumer preferences, enhancing the shopping experience and purchase likelihood [18]. The ThirdEye system utilizes smart glasses integrated with inertial sensors to track physical browsing in retail, which can optimize store layouts and improve the overall shopping experience [67]. Retail stores can also deploy a low-energy Bluetooth indoor positioning system to track consumers' paths efficiently and improve decision-making in retailing [74]. RFID readers integrated into smart shopping carts and smart shelving can streamline billing and enhance inventory management by attaching RFID tags to products [47, 71]. Smart shelves also use image recognition systems and sensor-based systems to analyze benefits, costs and planned developments, offering the most suitable solutions for retailers [43]. In addition, a smart shopping cart system can allow customers to scan items and view product details on the cart screen by interactive GUI, offering service assistance and minimizing shopping time [19]. Compared to others, we take a step forward in the smart capabilities of retail self-checkout systems by developing functionality to promote sustainable practices.

3 LIMITATIONS OF CURRENT SOLUTIONS

Consumer quality assessments primarily rely on visual assessment by the naked eye [66]. However, this method falls short of capturing the true quality of the produce. Computer vision can be used to automate visual assessment, but it is also unable to evaluate the true quality of a produce. To further motivate the need for enhanced solutions for quality estimation, we first highlight the constraints of both manual and automated visual assessment techniques.

3.1 Manual Inspection

To assess challenges in manual inspection, we conducted a two-week survey at a local university, engaging 60 participants (31 males, 29 females) across classrooms, offices, and the university canteen. Each participant examined a basket of seven organic produce items thoroughly (passion fruit, plum, apple, tomato, mandarin orange, mango, and melon) and rated their quality on a five-point Likert scale (1: strongly disagree – 5: strongly agree) in response to a closed-ended question (e.g., *"Is this tomato of good quality to eat?"*). Additionally, two open-ended questions explored shopping habits, inquiring about time from purchase to consumption (*"On average, how soon will you consume the produce that you purchase?"*) and strategies for assessing fruit quality. Completing the survey took on average 10 minutes. Participation was both anonymous and voluntary. To capture variations in internal quality, we employed the same set of produce throughout the two-week study, and restricted the number of respondents per day. Freshly procured at the start, the produce was consistently stored in the same room between the assessment days. Surveys were conducted on six evaluation days with 10 participants each, strategically aligned with key decomposition stages: day 1 (fresh), days 6, 8, 10 (active decay), and days 12, 14 (advanced decay). This approach provided insights into the accuracy and challenges in produce quality assessment. The produce items were deliberately chosen to represent commonly purchased items that pose significant challenges for manual inspection. As produce undergo decomposition, micro-bacterial proliferation ensues, leading to the softening of produce and eventually into visual alterations. The produce categories chosen for the study have thicker epicarp (skin) which delays the occurrence of visual alterations, which makes manual inspection challenging.

Results: To estimate the accuracy of manual inspection, we compared the subjective ratings given by the participants with the decomposition stage of the produce. Table 1 reveals that produce received improved scores despite the stage of advanced decay. A notable exception is the plum due to the softer skin, which exhibited clear visual alterations that participants correctly identified. In contrast, the other produce lacks such visual cues, resulting in minimal differences in quality assessments across the study period, highlighting the limitations of manual inspection. It is important to emphasize that these results were designed to shed light on the challenges inherent in manual inspection, rather than perform rigorous assessment of inspection accuracy. For example, we acknowledge that some produce may not have been fully ripe on day one despite being freshly procured from a supermarket, and hence the quality potentially is better on day 6 and 8 than on day 1. However, as the study spanned two weeks, this effect would not extend to the end of the second week, therefore not accounting for the observed results.

In terms of purchase habits, most participants made independent purchase decisions (80%) and consumed produce within the first five days (85%). This contrasts sharply with the quality assessments, where even the two weeks old produce items were deemed fresh. Participants prioritized appearance and color (95%) in quality assessments, followed by taste and smell (75%), texture (60%), and estimated nutritional value (33%). Several comments from participants revealed a reliance on touch and smell in the absence of visual cues. However, it became evident that subjective preconceptions often influenced the estimations rather than them being based on actual produce quality. For instance, participants associated hardness with unripeness and softness with ripeness, with some accurate and some misleading outcomes. For example, soft mango was correctly deemed ripe whereas a tomato was deemed ripe on day 14 due to its smell and softness despite already starting to rot. In summary, the survey results underscore how participants utilized simple heuristic principles for produce quality assessment, which, while sometimes accurate, could also be highly misleading. This reliance on heuristics transcends also to the retail environment, potentially resulting in consumers purchasing produce that are at the end of their life-cycle or that do not meet the consumers' expected quality assessments. Both of these issues lead to consumers discarding produce, contributing to elevated levels of food waste and loss. Offering an alternative method that accurately reflects the actual state of produce can mitigate these challenges and reduce unnecessary waste. Our work introduces an innovative technique that leverages human touch interactions to capture produce's internal state. This approach offers a more reliable and accurate solution for produce quality assessments.

3.2 Estimation Using Computer Vision

Automated visual assessment using computer vision [8] is the primary automated solution for quality assessment. We next illustrate that this approach encounters the same limitations as manual inspection, rendering it inadequate for supporting customers. We evaluate computer vision using 294 images captured over the same 14-day period as our survey (see Section 5), covering three produce items from the same seven categories. Images are labeled by decomposition stage: fresh (days 1-5), active decay (days 6-10), and advanced decay (days 11-14). It is important to note that these labels are not intended to precisely characterize produce quality but to signify the quality trends and help highlight the challenges associated with computer vision. We assessed five widely-used deep learning models: DenseNet201, InceptionV3, MobileNetV3large, ResNet50 and Xception. To enhance the generality, we replaced the top-most dense layer with three fully connected layers (1024, 1024 and 512 neurons) to capture more complex relationships. Pretrained weights from ImageNet were leveraged to configure the parameters of the convolutional layers to capture a broad set of visual cues, while separately learning the weights of the dense layers using the training data. The evaluation employed 5-fold cross validation, with images standardized to a common 300×300 resolution and augmented via random angle rotation, vertical and horizontal flips, and width and height shift changes. The augmented training dataset comprised 18 884 images (15 108 for training, 3776 for validation). Training utilized a batch size of 512 images and 100 epochs. Early stopping was utilized to stop training if validation accuracy stagnated for 10 consecutive epochs.

Despite the diversity and complexity of the model architectures, the best performing model achieved only 48% accuracy in predicting the decomposition stage. The lack of visual cues in the images, aside from plum as discussed previously, contributed to this limitation. While potential enhancements could be made to the model structure, the primary issue remains: visual cues are insufficient for accurate quality assessment. This is not to argue that computer vision techniques are not suitable - indeed, they are widely used during other produce life-cycle stages, e.g., packaging can use computer vision to identify diseases or defects [37]. However, these methods are inadequate for the retail environment as the available visual cues are insufficient for accurate quality

Table 1. Statistical rank of the fruit quality evaluation: 5-strongly agree and 1-strongly disagree.

Produce	Stage 1	Stage 2			Stage 3	
	Day-1	Day-6	Day-8	Day-10	Day-12	Day-14
Passion	2.6±0.9	2.2±1.0	2.6±1.2	2.7±1.1	2.1±1.1	2.3±0.9
Plum	3.6±1.5	2.5±0.9	2.6±1.7	1.2±0.4	1.2±0.4	1.7±1.0
Apple	**4.4±1.1**	**4.6±0.5**	**4.2±0.9**	**4.5±0.5**	**4.3±0.7**	**4.4±0.5**
Tomato	**4.0±1.1**	**4.1±0.6**	3.9±1.1	**4.1±1.2**	3.8±0.8	3.3±1.1
Mandarin	3.8±1.3	3.8±1.2	**4.0±1.3**	3.7±1.3	3.8±0.6	3.7±1.1
Mango	2.9±1.0	3.1±1.3	3.8±0.9	**4.4±0.5**	**4.5±0.5**	3.5±0.9
Melon	3.8±0.9	**4.0±0.8**	**3.8±0.6**	**4.0±0.8**	**4.1±0.9**	**4.1±0.9**

assessment. These results further emphasize the crucial need for novel and improved solutions for accurate produce quality estimation within the retail environment.

4 SNAKE DESIGN AND METHODOLOGY

SNAKE is an innovative, accessible, and cost-effective solution for estimating produce quality. It leverages heat transferred from human touch interactions [12]. Specifically, when customers touch produce, heat is transferred from their hands to the exterior surface of the produce. Once the interaction stops, the temperature begins to *dissipate* as the produce surface seeks equilibrium with the ambient temperature. The rate at which the heat decreases is referred to as the *dissipation rate*, which is the key variable that SNAKE monitors. This dissipation rate is directly linked to the internal characteristics of the produce (see Section 4.3), which correlate with changes in overall quality. Note that even a short interaction can result in a significant amount of heat transfer due to the difference between the produce's temperature and that of the human hand. As a result, dissipation time can differ significantly from the duration of the customer's interaction with the produce.

SNAKE employs a thermal camera to capture and monitor the rate at which thermal radiation dissipates, using these measurements to estimate produce quality. The key technical challenge addressed by SNAKE is accurately estimating produce quality from the transferred heat, as surface variations, distinct interaction patterns, and ambient conditions all affect heat transfer. Different types of produce also exhibit unique thermal properties that influence heat dissipation rates, necessitating adaptive modeling for consistent quality assessment. Additionally, external temperature fluctuations (e.g., between refrigerated and room environments) introduce further variability that must be accounted for.

SNAKE tackles these challenges with an innovative pipeline that accommodates variations in human touch patterns, including the size of the touched area and the duration of the interaction. The size is addressed by adaptively normalizing the monitored area, while the duration is managed using a two-phase approach with two linear regression models to normalize heat transfer to a consistent scale. Specifically, SNAKE incorporates a theoretical model of dissipation constructed from controlled measurements and estimates an empirical model from heat transferred during customer interactions of arbitrary durations. By correlating these models, our approach supports robust produce estimation from short (approximately 5 seconds) dissipation measurements, even when the theoretical model considers dissipation measurements collected over a longer time window. To enhance robustness further, SNAKE incorporates compensation models that account for hand temperature and environmental temperature variability, ensuring consistent performance across diverse conditions (more details in Sections 7 and 8).

4.1 SNAKE Overview

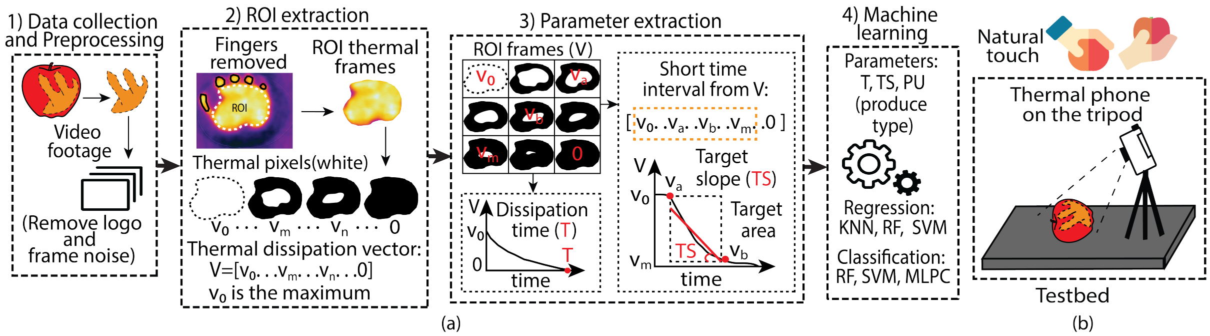

Fig. 2. a) Thermal imaging modelling pipeline; a, b, m, n are the frame timestamps during the thermal dissipation, $0<a<b<m<n<T$, b) Testbed.

Algorithm 1 Calculate Vector (V) From Hand Heat

Require: Frames from thermal footage
Ensure: Thermal dissipation vector (V)

```
1:  for each INPUT do
2:      image ← Conversion to Grayscale; Apply GaussianBlur, Threshold
3:  end for
4:  initialize V array
5:  for each i in images do
6:      x, y, w, h ← cv2.boundingRect() {heat coordinates}
7:      ROI ← image[y:y+h, x:x+w] {hand palm coordinates}
8:      thermalarea ← count white pixels(255)
9:      Add thermal value to vector V
10: end for
11: V ← Scale V, Sliding window V
```

SNAKE leverages heat transfer from touch interactions to estimate produce quality using a four-stage pipeline summarized in Figure 2 and elaborated in Algorithm 1. The first phase, *sampling*, involves collecting video footage from a thermal camera or a thermal array sensor. The second phase, *data processing*, extracts image frames from the video data and performs preprocessing on them. This preprocessing involves converting the images to greyscale using Gaussian blur and thresholding (Lines 1 - 3) to separate the produce item from the background. As touch interactions result in the produce item having differing thermal patterns than the ambient environment, this simple approach suffices for separating the foreground and background. The third phase, *parameter extraction*, converts the thermal fingerprint into a consistent representation and estimates the dissipation rate of the produce. Finally, the *modeling* phase employs machine learning using the extracted parameters as input to assess produce quality.

4.2 Robust and Accurate Parameter Extraction against Touch Variations

SNAKE requires robust and accurate estimates of the thermal dissipation values to estimate produce quality reliably. However, this is highly challenging as the amount of heat that is transferred to an item depends on the area that the hand touches and the duration of the interaction. We next detail how SNAKE overcomes these challenges.

To accommodate variations in the touch area, SNAKE extracts a region of interest (ROI) from the image frames and analyzes dissipation only within this area. The ROI corresponds to the part of a produce item that the user touched. Note that interaction force has a negligible effect on SNAKE as the size of the ROI only depends on the area that the user interacts with. Greater – or weaker – interaction force affects the contact between the produce surface. This can improve or decrease overall heat conduction, but does not affect the size of the area where this heat resides [12, 20, 40]. Indeed, by capturing the ROI, SNAKE measures the thermal response directly, allowing it to capture these variations in heat transfer without relying on predefined assumptions about force.

We extract the ROI by forming a bounding box around the area where the hand touched the produce item (line 6), and using contour detection to extract this area (line 7). To further enhance robustness, we also remove noise from the image frames by eliminating areas with low-intensity thermal radiation as these can be a result of reflections from other sources [69] or caused by weak or accidental touch interactions. Specifically, we eliminate thermal values that are outside of the 90% quantile of the distribution of thermal values within the bounding box. After preprocessing, we extract a dissipation vector V by calculating the reduction in ROI area compared to the previous frame (lines 8-9). Thermal dissipation time T is calculated from the reduction of the *white* area in the thermal fingerprint until it fully disappears (all *black*), indicating that the thermal value in the vector reaches zero. To make these values comparable against variations in touch area, we scale the dissipation values to a consistent scale. As the scaling can magnify low-intensity areas at the expense of high-intensity areas, we smooth the values with a sliding window filter [46] before scaling them. The filtering is done using one-second windows and it utilizes 50% overlap.

The parameter estimation also needs to cope with variations in interaction duration as these also influence the amount of thermal radiation that is transferred onto the produce item. SNAKE achieves this using a regression approach that converts observed interactions to a consistent scale and allows estimating the current state of the produce. This is accomplished using two regression models. The first uses the available image frames to estimate the dissipation slope, denoted LS (linear slope), which allows estimating the overall dissipation time from measurements that are available at that point. Linear slope LS is calculated based on common linear regression. The regression model for the target slope is incrementally estimated by threshold and re-updated after each frame. Separately, SNAKE integrates a second regression model that provides a reference for the dissipation slope at different stages of decomposition. We refer to this as the target slope, and denote it using TS. By comparing the current estimate LS with the reference TS provided by the target slope, the state of the decomposition can be estimated. Both regression models are obtained using linear regression, but we use robust regression for the target slope to improve model fit as short duration tends to cause more variance and can otherwise result in poor model fit. As an example shown in Figure 2(a), we consider a short-time interval of m frames from the dissipation vector V, where thermal values follow the sequence $V_0 > V_a > V_b > V_m$, with corresponding timestamps $0 < a < b < m$. The linear slope LS is estimated from the interval between timestamps 0 (dissipation start) to m. However, to ensure accurate dissipation rate estimation, we filter out frames where adjacent thermal value changes are minimal by threshold, as they do not effectively represent the dissipation process. The target slope TS is then updated and derived from the interval between timestamps a to b within the m frames. As part of the experiments, we also consider models that leverage produce type (PU) as input feature to see how tailoring the analysis to specific produce category can improve performance. Most existing solutions rely on produce category, and this information can be easily obtained either from user input or using computer vision.

4.3 Theoretical Background

Thermal radiation is electromagnetic radiation that results from changes in the thermal state of an object. This radiation is visible in the infrared part of the light spectrum [68] and can be captured using a thermal imaging device, such as a thermal camera or a thermal array sensor. The amount of thermal radiation that can be captured from the object depends on *emissivity*, denoted as ϵ, which indicates the fraction of thermal radiation the object emits or absorbs [54]. The higher the emissivity, the better thermal radiation can be captured. Organic materials and water both have high emissivity, making them conducive to thermal radiation capture.

A thermal footprint, also known as a fingerprint, refers to the distinctive pattern of thermal radiation an object emits, depicting how it differs from its surroundings. SNAKE captures these footprints and analyzes the rate at which they change over time to assess produce quality. This rate of change is referred to as *thermal dissipation* [17]. According to the laws of thermodynamics, any object will seek to reach a thermal equilibrium with its environment. Consequently, any thermal radiation decays over time and the dissipation rate characterizes the speed at which this decay occurs.

Water loss is a key factor affecting produce quality, as dehydration accelerates postharvest deterioration [52, 58]. It is often referred to as weight loss, mass loss, or moisture loss, as all three terms describe its direct impact on fresh produce [6, 61]. Water loss causes wilting, shriveling, and loss of firmness, diminishing both visual appeal and nutritional value [29, 32, 65]. This reduces consumer desirability and saleable weight while accelerating spoilage by depleting stored food reserves and increasing susceptibility to pathogens. Thus, effective moisture management is essential for preserving freshness, extending shelf life, and maintaining overall produce quality.

Fresh produce has a high water content which decreases over time due to transpiration and causes the fruit pulp to lose firmness and eventually to decay. As water has high emissivity, this means that the amount of heat the produce emits from its interior to the exterior decreases as the produce decays. The pace of the transpiration process within a produce can be characterized by three thermal properties [42, 57]: thermal conductivity k, thermal diffusivity α, and specific heat capacity C_p [51, 56]. Thermal conductivity signifies the rate at which heat traverses the fruit, while thermal diffusivity quantifies the material's heat-conducting ability relative to its heat storage capacity. Heat capacity determines the amount of energy required to raise the temperature of the produce incrementally (one kilogram by one degree). As these parameters are directly linked with water loss, they are also indicative of the changes we expect to see in thermal radiation and its dissipation. For example, high water content leads to faster thermal transfer from the produce's interior, resulting in distinct changes in the thermal fingerprints.

In parallel to the internal changes, the exterior of the produce may be softer or undergo other alterations that can affect its emissivity. Together these two behaviours change the dynamics of thermal transfer over time, and SNAKE builds on the idea of monitoring and capturing these changes. As will be shown in the evaluation, changes in the dissipation fingerprints reflect these changes and enable accurate estimation of the actual produce quality.

5 EXPERIMENTAL SETUP

We evaluate SNAKE through rigorous and systematic experiments that account for the decomposition of fresh produce. Due to the limited shelf life of produce, our evaluation incorporates independent studies conducted over time with the same items. In addition to an in-depth analysis of SNAKE, we compare its performance against two state-of-the-art baselines that use alternative sensing modalities. We next describe our experimental design and procedure as well as the baselines we compare against.

5.1 Experimental Design

Procedure: Our primary experiment considers produce quality estimates measured each day over a 14− day period by two participants, referred to as P1 and P2. We additionally conducted small-scale follow-up tests which focused on assessing the generality of our approach. These measurements are described as parts of the results in Section 6.7. In our experiments. we consider seven different types of produce, corresponding to fresh produce that are commonly available and purchased from supermarkets and covering the 5 primary categories of produce [89]: pepo (melon, passion fruit), pome (apple), berry (tomato), drupe (plum, mango) and hesperidium (mandarin orange). As discussed in Section 3.1, we focus on most produce with thicker epicarp as these are the most difficult ones for visual inspection and generally result in the highest amount of misclassifications by the consumers and potentially by the retail staff. To assess variation within produce of the same category, we consider three items from each category, selecting items with different sizes and shapes, but with a similar visual appearance. Thus, in total 21 items were used.

Prior to starting the experiment, the fruits being measured were first placed into clean baskets where they were kept until they had attained thermal equilibrium with the room's temperature. Each produce was kept in a separate basket to ensure there was no thermal transfer between produce in the experiments. Both participants then interacted with each of the 21 produce by holding them for 60 seconds (long interaction) and 10 seconds (short interaction). Interaction time refers to the duration the produce is held. Once the time had elapsed, the participants placed the fruit on a testbed where different measurements were collected (see below). The participants were free to choose the produce in any order they preferred and they interacted with the produce naturally using their dominant hand. The long and short interaction duration emulate differing interaction patterns with the former corresponding to a careful examination of the produce and the latter for a brief and superficial inspection. Our prior work has shown that 10 seconds is sufficient for estimating thermal dissipation patterns [17], whereas the longer interactions offer an opportunity to assess statistical variation within the samples. To ensure consistent measurements, we used a clinically certified contactless optical thermometer (DR CHECK FC500) to verify that the skin temperature of the participants conducting the experiment was normal prior to having them interact with the produce. We also assessed the palm temperature of the participants using a thermal imaging scanner (FLIR TG267) before touching the produce. These measurements were used to assess the effect potential variations in hand temperature have on the results.

Testbed and Measurements: Measurements were collected using a controlled testbed, illustrated in Figure 2, located within a single room. We used the same room throughout the experiments to minimize external variation from different environmental conditions, and to ensure the thermal measurements can be reliably compared across days and produce items. The testbed consisted of a FLIR-capable smartphone (Caterpillar CAT S61) which was placed on a tripod at approximately 30 cm distance from a table with a black background and surface. The black background allows obtaining clean video footage of the thermal footprint without influencing the thermal radiation emitted by other objects in the surrounding environment.

Once the produce item was placed on the testbed, video footage of thermal dissipation was recorded using the thermal camera of the CAT S61 smartphone. The camera has internal calibration which was triggered prior to starting the recording. Thermal dissipation time was estimated automatically from the thermal video and validated by comparing it to a ground truth obtained from manual inspection with a stopwatch. To ensure consistent ambient conditions, we recorded the ambient temperature (23°C−23.8°C) and relative humidity (32 ± 2.24%) of the room where the testbed was located. These measurements were collected using a Netatmo portable weather station. Additionally, once the thermal dissipation measurements were collected, we used our two baselines (optical sensing and wireless sensing; see below) to measure the items. Finally, a picture of the produce was taken at the end of the experiment. These images were also utilized in Section 3.

Ground Truth: Ground truth for the produce was obtained using a durometer to record the firmness of each fruit. Firmness refers to the softness or hardness of the produce and it is commonly used as an indicator of produce quality [80]. Firmness can be affected by water (mass) loss as decomposition initiates. This influences the internal thermal properties of produce, contributing to superficial changes [35, 61]. Water loss and firmness changes rates are commonly interconnected. Thus, SNAKE builds the relation between the thermal imaging and produce firmness by looking at the water loss rate. The durometer readings were taken three times per day and averaged to obtain a firmness score for each produce. As the durometer we used the commercial fruit hardness tester (Turoni 53215TP) which has a measuring capacity of 90 shore. While the durometer manufacturer states the device to be non-invasive, in practice it requires contact with the surface of the produce item. This could cause damage to the skin of the item, thus accelerating decay. To ensure this is not the case, we took firmness measurements only from two of the items (referred to as S1 and S2) and used the third item as a reference to compare potential effects on thermal dissipation across days. No statistically significant differences in thermal dissipation were observed across the three items, validating that the durometer had no impact on produce decay. We also measured the fruit mass (in grams) using a kitchen scale.

Ethics: The experiments were given ethical approval by the IRB of University of Tartu and all participants recording the measurements gave their informed consent to allow using their measurements.

5.2 Baselines

As part of the experiments, we compare SNAKE against two baselines, elaborated below. The measurements for the baselines were collected simultaneously as we recorded the thermal footage.

Optical Sensing (Baseline 1): We compare the performance of SNAKE against a state-of-the-art optical sensing solution [89]. This approach relies on a green laser diode and a photoresistor to measure reflected light from the produce's surface. We consider reflectivity analysis of fruits using the photoresistor connected to the analog input pin of an M5StickC PLUS ESP32 development board, which integrates Wi-Fi and Bluetooth capabilities. The M5StickC PLUS controls the sampling frequency (5Hz) and uploads the samples to a Web server. The photoresistor captures light changes based on its resistance exposure to the light intensity of the reflected material and this information is stored on a Web server. The distance between the sensor and fruit is within one centimeter, and two random 1-minute measurements per fruit are taken to mitigate the potential biases.

Wireless sensing (Baseline 2): We also compare the performance of SNAKE against state-of-the-art wireless sensing solutions [49, 77]. We measure the Channel State Information (CSI) of WiFi signals (2.4GHz frequency and channel six), which carry information about the propagation characteristics of radio signals. When the radio signals traverse through the produce, the signal characteristics, e.g., amplitude, phase; are affected by the produce's interior composition, which can be used as input to estimate ripeness. We use two ESP32 microcontrollers: active access point (AP) as the transmitter and active station (STA) as the receiver, since they are small and easy to deploy. The distance between the AP and STA was set to 20cm, so placing a fruit between them could block the line-of-sight (LOS) of the WiFi signals. Two random 1-minute measurements are also considered.

To pre-process the WiFi data, we first denoise the signals using convolution-based filtering. We then form frames from the measurements using a one second sliding window with 50% overlap. To identify the most relevant parts of the signal, we use principal component analysis (PCA) on the data and use the three top-most principal subcarrier components to represent the measurements. We opted for three principal carriers as over 90% of all information was contained by them. We then separate the low and high frequency components of the signal using Daubechies 2 discrete wavelet transform to separate the low and high frequency components for both CSI amplitude and phase. We average the low frequency components of the amplitudes and use them as the main feature as the average value of the high frequency components is close to zero. Also the phase information

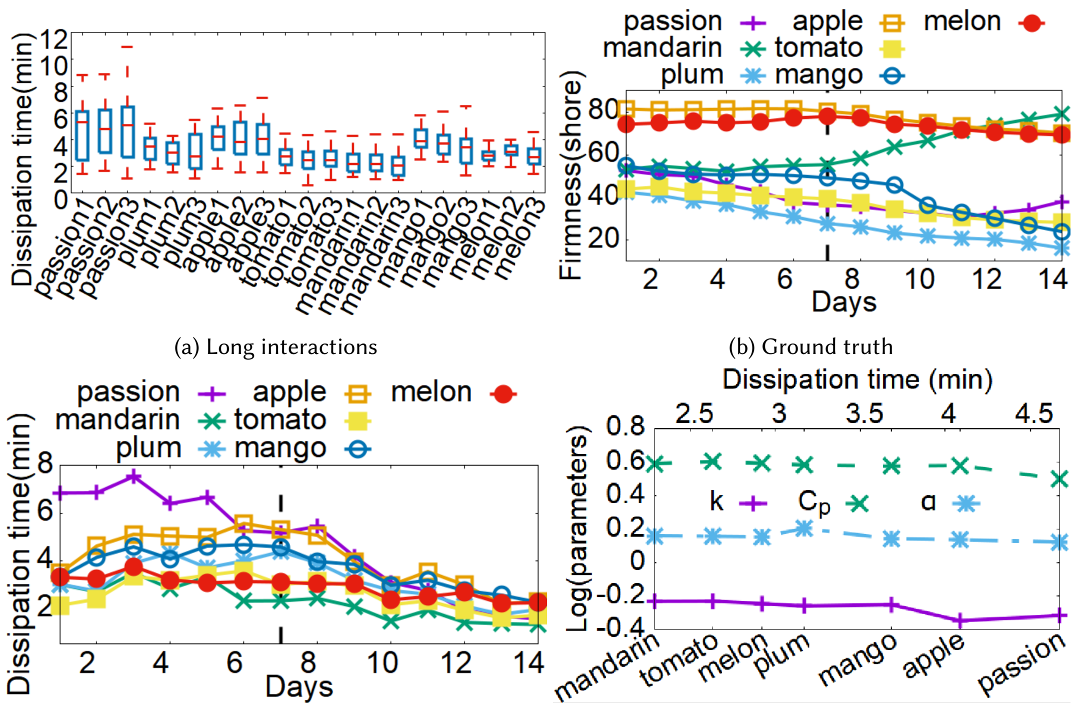

(a) Long interactions

(b) Ground truth

(c) Long interactions

(d) Thermal properties

Fig. 3. Evaluation results in long interactions (1-min touch). (a) Thermal dissipation time of each produce. (b) Firmness value for each produce as given by the durometer. (c) Thermal dissipation time of different produce across the 14− day period. (d) Relationship between thermal properties and the mean dissipation time, k, α and C_p as mentioned before.

largely captures dynamic oscillations in the environment rather than static effects caused by the composition of the produce.

6 RESULTS

6.1 Thermal Dissipation Time as a Proxy for Decomposition

SNAKE relies on thermal dissipation measurements to estimate produce quality. The measurements are used as a proxy for internal changes taking place inside the produce, which in turn characterize decomposition and the quality of the produce. We begin our evaluation by validating the use of thermal dissipation measurements, demonstrating that they can be used to characterize different produce and that they correlate with gold standard estimates as measured by a durometer. For details on the experimental setup we refer to Section 5.

Figure 3(a) shows the thermal dissipation distribution of different produce items, averaged across the experiment duration (i.e., 14 days). From the figure we observe that the differences between produce items are larger than differences within items of the same produce category. Krusal-Wallis tests were used to verify that the differences in thermal dissipation are significant for all the produce ($\chi^2 = 141.99$, $\eta^2 = 0.23$, $p < .05$), This implies that thermal dissipation can reliably characterize different produce categories. When comparing individual produce, the surface characteristics of the produce affect the variation in thermal dissipation. Specifically, produce that undergo clear surface changes have higher variance in thermal dissipation (e.g., mango and passion fruit) whereas those that undergo fewer surface changes are more stable over time (e.g., melon). Pairwise post-hoc comparisons (Dunn-Bonferroni) of the thermal dissipation time indicated significant differences in all but two cases: plum and melon ($\chi^2 = 1.10, p > .05$) and apple-passion fruit ($\chi^2 = 0.27, p > .05$). This indicates that thermal dissipation time generally distinguishes between different fruits, but may struggle with specific produce that have similar surface characteristics. In these cases, additional measurements are needed to estimate fruit type robustly.

Figure 3(b) shows changes in firmness for the produce across the 14 day experiment period, indicating that most produce decompose approximately within a week at which point a significant drop in firmness can be observed. The hardness of the produce skin affects the decomposition speed with mandarin orange and passion fruit having slightly slower decomposition due to their harder epidermis. To compare the firmness values with thermal dissipation, Figure 3(c) shows the average dissipation time of all fruits for 14 days. On visual inspection, the thermal dissipation time follows the same trend as the firmness values. To verify that these patterns are meaningful, we calculated the (Kendall τ) correlation between thermal dissipation time and changes in produce firmness. The correlation is strong (92.86% of all fruits), confirming that dissipation time correlates with changes in firmness, which is a widely used indicator of produce quality [1]. We separately calculated the correlation between thermal dissipation values and produce mass, which was similarly found to be strong and very significant (95.23%). Both firmness and mass are commonly used to characterize produce decomposition processes as they capture internal changes (e.g., thermal properties) taking place within a produce [31, 57]. Finally, we calculated the correlation between thermal dissipation time and three distinct thermal properties: thermal conductivity, thermal diffusivity, and specific heat capacity (see Section 4.3). In particular, we rely on typical values of these thermal properties [21, 26, 27, 31, 41, 57]. The Kendall correlation verified a statistically significant relationship between thermal dissipation time and these three parameters (for all parameters, $\tau < -0.71, p < .05$). Hence, our results demonstrate that thermal dissipation measurements can serve as proxy for internal changes taking place inside the produce. As we consider produce from all main fruit categories, this finding also demonstrates that SNAKE generalizes across distinct decomposition patterns. Specifically, while the most common decomposition pattern is softening of the produce exterior over time, there are also produce for which the surface hardens after an initial softening phase (e.g., mandarin).

As the durometer requires contact with produce skin, we additionally compared the thermal dissipation values of the item (S3) for which durometer was not applied to the items that were measured with the durometer (S1 and S2). There were no significant differences in within-produce variation, as confirmed by Friedman tests ($p > 0.05$). This indicates that the durometer does not cause significant damage to the produce surface and that the firmness and thermal dissipation values can be reliably compared across the entire period.

6.2 SNAKE Performance

We next use our measurements to evaluate the overall performance of SNAKE by comparing the estimates derived from thermal dissipation values with measurements provided by the durometer. We first conduct classification experiments to obtain a coarse-grained indication of performance. We then supplement these with regression experiments that compare changes in thermal dissipation with changes in firmness, as measured by the durometer.

Classification for Coarse-Grained Quality Assessment: We first consider classification experiments where we categorize the fruits into the three common ripeness classes: fresh (L0), active decay (L1) and advanced decay (L2). These labels are intended to capture trends in produce quality and to offer a way to obtain a coarse-grained assessment of performance, not to characterize produce quality precisely. We categorized the measurements into these classes using clustering based on the firmness values. We separately consider short (10 second) and long (1 minute) interactions to assess how the measurement window affects performance. As classification techniques we consider three simple yet common machine learning techniques: Multilayer Perceptron (MLP), Support Vector Machine (SVM), and Random Forest (RF). The input features for all classifiers were the thermal dissipation

Table 2. Regression predicting firmness (F); Features: Thermal dissipation time (T), Target dissipation slope (TS), Produce type (PU). –: misinterpretation

Sensing modality	Features	Day1/2	Day3/4	Day5/6	Day7/8	Day9/10	Day11/12	Day13/14	5-CV	
		RMSE	RMSE	RMSE	RMSE	RMSE	RMSE	RMSE	RMSE	R^2
Long interactions	**(T)**	0.263	0.285	0.274	0.304	0.321	0.330	0.344	0.293	–
	(T,PU)	0.141	0.080	0.060	0.072	0.095	0.125	0.135	0.092	0.895
Short interactions	**(TS)**	0.262	0.248	0.301	0.283	0.272	0.328	0.335	0.263	0.151
	(TS,PU)	0.085	0.098	0.089	0.091	0.090	0.085	0.141	0.084	0.913

time, target slope, and produce category. Features were normalized using min-max normalization, and one-hot encoding was used to assign labels for samples. As evaluation metric we use classification accuracy which was calculated using a 5-fold cross-validation.

When only thermal dissipation is considered, the average estimation accuracy is relatively low for both interactions (short: 57.15%, long: 54.86%). This corresponds to a generic model when no information about the produce is given. Once we consider the produce type, the average performance of SNAKE improves for both short (average: 73.13%) and long interactions (average: 73.65%). The differences between 10-second and 1-minute interactions were not found to be statistically significant, suggesting that SNAKE can reliably estimate quality from interactions with different duration. Figure 4(a-b) shows the confusion matrix of the SVM classifier. The misclassification mainly happens between adjacent ripeness classes, which can be mitigated by improving the granularity of the labels. Indeed, as the labels were assigned using clustering, the borders between adjacent labels are not clearly distinguishable. The results from regression experiments below further support this view, demonstrating consistently low error and good model fit.

Regression-Based Quality Assessment: To obtain a more fine-grained estimate of SNAKE's potential for assessing produce quality, we performed regression experiments that assess the potential of thermal dissipation being able to estimate firmness, a key indicator of produce quality. As in the classification experiments, we separately considered short and long interactions. Similarly, to the classification experiments, we focus on simple techniques as these would be easier to deploy in practical use: K-Nearest Neighbor (KNN), Support Vector Regression (SVR), and Random Forest (RF). As evaluation metrics we consider the average root mean square error (RMSE) which was calculated using two different cross-validation approaches: a 7-fold cross-validation where two successive days are combined into a fold, and a time-independent 5-fold cross-validation.

Table 2 shows the average root mean square error RMSE for each regression model and the R^2 score for each interaction. We can still observe poor performance when only considering the thermal dissipation, as the models cannot identify the characteristics of each produce. However, after adding the produce type information, SNAKE consistently performs well, capturing a high amount of variance (short interaction: RMSE=0.084, R^2 = 0.913). The performance between short and long interactions was similar, and no statistically significant differences were observed. Figure 4(c-d) also shows that the true values and predicted values are mostly distributed along a linear line, indicating accurate firmness estimation for SNAKE.

While the fit of the regression line is generally good, for some produce the errors remain somewhat higher which is mostly due to differences in produce surface characteristics. The most notable cases are the plum and the mandarin orange as can be seen from the variation around the diagonal. In Section 7 we demonstrate how to further improve produce estimation performance by harnessing information about palm temperature variations.

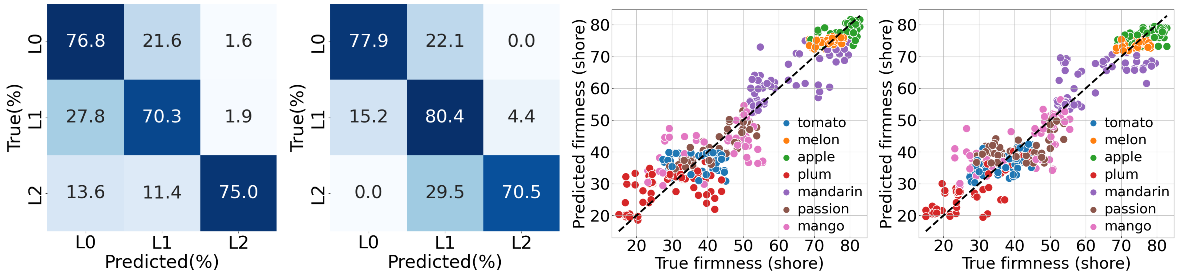

(a) Long interactions(1min) (b) Short interactions(10sec) (c) Long interactions(1min) (d) Short interactions(10sec)

Fig. 4. SNAKE performance by considering the thermal dissipation and produce type, (a)-(b) classification, (c)-(d) regression.

Table 3. Regression predicting firmness (F) and classification performance for baselines and SNAKE; Features: light value (L), CSI amplitude (A), Produce type (PU), Thermal dissipation time (T), Target dissipation slope (TS). −: misinterpretation.

Sensing modality	Features	Day1/2 RMSE	Day3/4 RMSE	Day5/6 RMSE	Day7/8 RMSE	Day9/10 RMSE	Day11/12 RMSE	Day13/14 RMSE	5-CV RMSE	5-CV R^2	5-CV Classification	SNAKE	Features	5-CV RMSE	5-CV R^2	5-CV Classification
Optical sensing	**(L)**	0.282	0.230	0.260	0.268	0.286	0.295	0.334	0.262	0.155	44.72%	**Long interactions**	**(T)**	0.293	–	54.86%
	(L,PU)	0.185	0.133	0.101	0.074	0.093	0.126	0.183	0.107	0.870	56.8%		**(T,PU)**	0.092	0.895	73.65%
Wireless sensing	**(A)**	0.245	0.240	0.277	0.286	0.309	0.327	0.352	0.294	–	47.45%	**Short interactions**	**(TS)**	0.263	0.151	57.15%
	(A,PU	0.172	0.135	0.083	0.061	0.079	0.146	0.191	0.119	0.842	52.13%		**(TS,PU)**	0.084	0.913	73.13%

6.3 Comparison to baselines

We next compare SNAKE with state-of-the-art baselines leveraging optical and wireless sensing (see Section 5) and demonstrating the superior performance of SNAKE.

Table 3 compares optical sensing and wireless sensing against SNAKE. While all systems benefit from produce information, SNAKE consistently outperforms the baselines in both classification and regression tasks. In classification, optical sensing achieves an average accuracy of 56.8% whereas wireless sensing achieves an average accuracy of 52.13%, which is significantly lower than the ≈ 73% classification accuracy achieved by SNAKE. For regression the findings are similar. Specifically, optical sensing achieves slightly better performance (RMSE = 0.107, R^2 = 0.87) than wireless sensing (RMSE = 0.119, R^2 = 0.842), but both baselines are significantly worse than SNAKE (short interactions: RMSE=0.084, R^2 = 0.913). When produce information is not available, the performance of SNAKE remains reasonable whereas the performance of optical sensing and wireless sensing drops considerably, explaining only $10-20\%$ of variation. This demonstrates that SNAKE achieves robust performance across different application scenarios, emphasizing the versatility and robustness of SNAKE compared to baselines. To better understand the performance of the baselines, Figure 5 shows the results of the regression experiments for both optical sensing and wireless sensing. Optical sensing performs well with produce that have clear surface changes, such as plum, whereas wireless sensing shows significant variations across all produce. In contrast, as we have shown, SNAKE operates consistently across most of the produce.

To gain deeper insights into the performance of optical sensing, Figure 6(a) illustrates the standard deviation of light reflection measurements over the 14-day data collection period. The deviation of the reflected light measurements remains relatively stable across the days, with the apple being the only exception. This variability can be attributed to significant changes occurring on the surface of the apple compared to other produce. Indeed, visual inspection of the collected images reveals substantial alterations in the surface color of the apple, with differences in pigmentation being the primary cause of variations in the light values. Figure 6(b) displays the mean absolute deviation for all produce. The measurements of the three samples of the same produce were averaged to

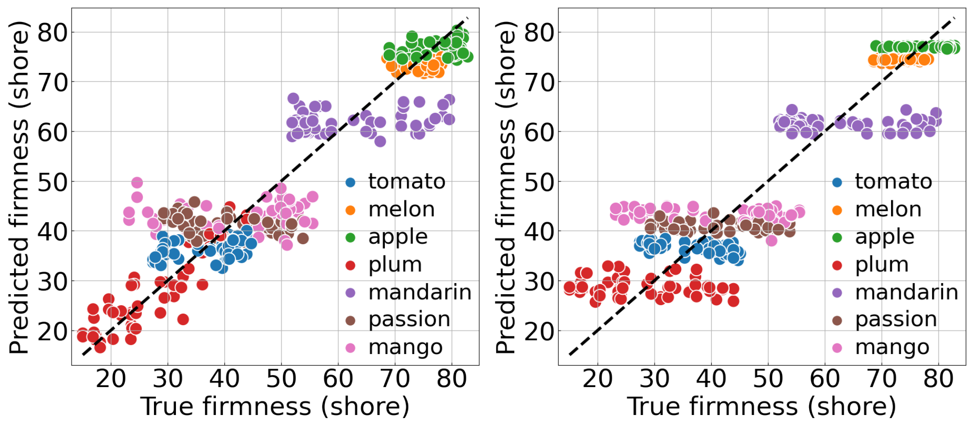

(a) Optical sensing (b) Wireless sensing

Fig. 5. Fruit firmness estimation performance considering sensing information and produce type.

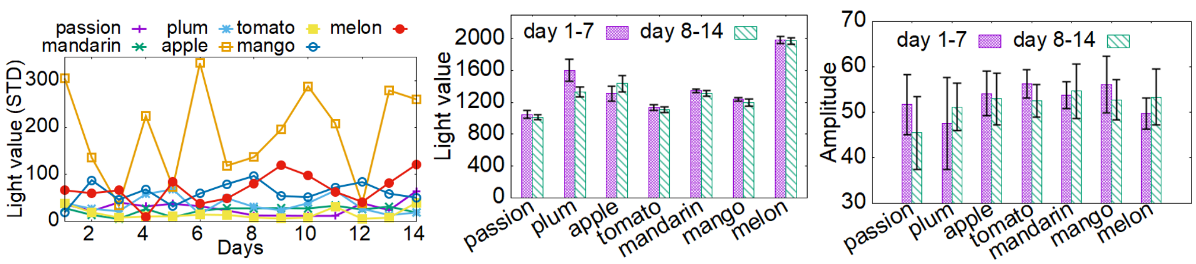

(a) Optical sensing (b) Optical sensing (c) Wireless sensing

Fig. 6. a) STD from 3 samples per fruit, b) MAD of light values, e) MAD of wireless amplitude.

obtain a more robust estimate for each produce type. Subsequently, the data was divided into separate sets for the first and last seven days to estimate the average light values. The figure illustrates that the most significant changes occur for plum, whose surface softens during the decomposition process, while other produce show smaller variations in light measurements. Although optical sensing can track decomposition across different produce types, its overall performance is contingent on the sampled area of the produce. Since optical sensing utilizes a beam of light for sampling, a single sample may not sufficiently represent the overall quality. In contrast, SNAKE overcomes this limitation by sampling a larger surface area using natural human interactions.

We also conducted a similar analysis for wireless sensing. Figure 6(c) illustrates the mean absolute deviation for the low-frequency components of the CSI amplitude. The differences in the mean values between the first and last seven days can be more accurately quantified compared to optical sensing. However, we observed higher variations in the samples taken on different days. This suggests that while it is feasible to identify the produce to some extent, identifying its decomposition state and quality may be challenging. Wireless sensing requires a specialized measurement setup involving the physical deployment of transmitters and receivers, as well as stringent control of the measurement setup to ensure accurate estimations. Wireless sensing is also heavily influenced by the surrounding context, indicating impracticality for real-world deployments. In contrast, SNAKE

Table 4. Weight of variables to fit linear slope (LS) in long interactions. Variables: produce mass (M). Total means the thermal dissipation time.

Intervals	first 1s	first 5s	first 10s	first 20s	first 30s	first 40s	first 50s	first 60s	Total
M	-1.12	-3.85	-3.65	-3.64	-3.92	-4.08	-4.18	-4.23	-3.57
R^2	0.20	0.30	0.40	0.51	0.63	0.68	0.71	0.71	0.68

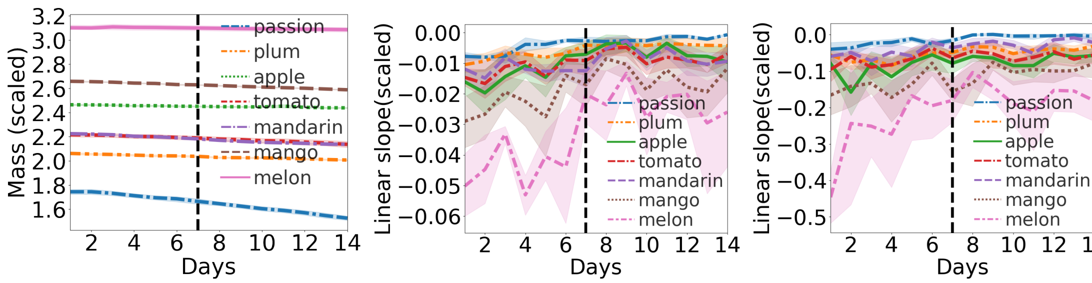

(a) All fruits (b) Long interactions (c) Short interactions

Fig. 7. a) Fruit mass decreases over days, b) Linear slope with 95% CI for all items when considering the first 40s from the thermal dissipation, c) Linear slope with 95% CI for all items when considering the first 5s from the thermal dissipation

Table 5. Weight of variables to fit linear slope (LS) in short interactions. Variables: produce mass (M). Total means the thermal dissipation time.

Intervals	first 1s	first 2s	first 3s	first 4s	first 5s	first 6s	first 7s	first 8s	first 9s	first 10s	first 15s	Total
M	-7.45	-18.17	-23.67	-26.18	-26.65	-26.41	-25.93	-25.36	-24.63	-23.94	-20.47	-9.55
R^2	0.31	0.45	0.55	0.60	0.68	0.68	0.70	0.70	0.72	0.71	0.68	0.68

utilizes heat transmitted from the user's hand to the produce. As the intervals of body temperature do not change considerably between individuals, SNAKE can be readily adapted for diverse contexts and interactions.

6.4 SNAKE and Interactions with Different Duration

Our results thus far have demonstrated that SNAKE accurately estimates produce quality, outperforming state-of-the-art baselines. These results were obtained using interactions with a fixed duration (10 seconds or 1 minute), and generalizing to touch interactions with arbitrary duration is also essential for the practicality of SNAKE. In this section we further scrutinize short and long interactions, and demonstrate that using the slope of the thermal dissipation makes it possible to estimate produce quality from interactions with a different duration.

Table 4 analyzes the relation between linear slope (LS) estimate obtained from thermal dissipation measurements of long interactions and produce mass (M). In the analysis, we consider different windows for analyzing the dissipation time to understand the effect the duration of the thermal footage has on estimation. From the table, and as also illustrated in Figure 7, we observe that the longer the footage of dissipation, the stronger the relation between the linear slope and produce mass. The relationship saturates at around 40 seconds (R^2 = 0.68) with longer intervals resulting only in minor improvements. The weight of the regression is negative, which means that the speed of thermal dissipation (i.e., higher value of slope) increases as produce mass decreases.

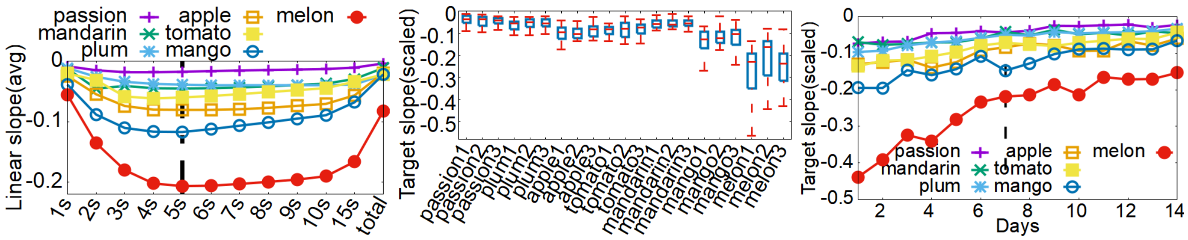

(a) Short interactions (b) Target slope (c) Target slope

Fig. 8. a) Average linear slope (scaled) in different time intervals of the thermal dissipation, b) Target slope over 14 days, c) Average target slope for all fruits.

Table 5 shows the corresponding results for short interactions, considering dissipation intervals from 1 to 15s. Note that the analysis is done on the dissipation measurements induced by the interactions, which allows us to use a longer interval than what the interaction duration was (i.e., 10 seconds for short interactions). As with the long interaction data, the fit of the model improves with larger intervals. The model fit is good from around 5 second onward ($R^2 = 0.68$), improving until around 10 seconds, after which the fit starts to decline. As with the long interactions, the relationship between slope and produce mass is still negative, confirming consistency of the pattern, see Figure 7.

Interactions with short duration are easier to capture in practice, and we next analyze the 5 second dissipation intervals in more detail, see Figure 8(a). Overall, the first 5 seconds capture over 50% of the overall thermal dissipation compared to initial values. Therefore, estimates of produce quality can be obtained from thermal dissipation lasting at least 5 seconds. Despite its utility for produce quality estimation, the linear slope may exhibit local irregular oscillation for some fruits, such as melon in Figure 7(c). Figure 8(b) shows the target slope estimated from the first 5 seconds for all fruits in short interactions. We can observe that the different fruits have distinct slopes. We also verified (using Kruskal-Wallis tests) that these differences are statistically significant ($\chi^2 = 315.27$, $\eta^2 = 0.53$, $p < .05$). We used Friedman tests to compare samples of the same produce and with one exception the target slopes of distinct samples of the same produce were not significantly different ($p > 0.05$). The only exception is the melon, which is due to variations in palm temperature affecting the thermal transfer and consequently also dissipation patterns. We demonstrate this in Section 7 and also extend SNAKE by presenting a compensation model that overcomes this issue. Moreover, Figure 8(c) shows that the target slope follows similar trends as the firmness obtained by the durometer. The pattern of the target slope is also consistent with the linear slope analysis for all fruits. Overall, the results indicate that the target slope captures fruit decomposition accurately.

To demonstrate the use of the slope, we carry out a small-scale follow-up experiment where we consider a fresh set of produce covering the main categories (one sample per fruit type) and vary the touch time considering the following values: 1s, 5s, 10s, 15s, 30s and 1min. Figure 9(a) shows the average dissipation time with different touch periods. The differences between the fruits are consistent, and the dissipation values increase approximately linearly as touch time increases. The corresponding changes in the slope are shown in Figure 9(b). For fruits with a harder exterior, the slope is consistent across time, whereas those with a softer exterior absorb more thermal radiation and the speed of dissipation depends on the extent of radiation that is absorbed by the fruit. The saturation point comes between $5 - 10$ seconds, after which the magnitude of the slope consistently decreases. This effect is clearly also visible in the dissipation values and thus the slope and the dissipation values complement each other and support robust produce quality estimation with touch interactions having different durations. In

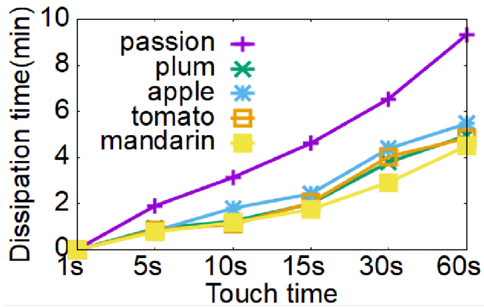

(a) Random touch

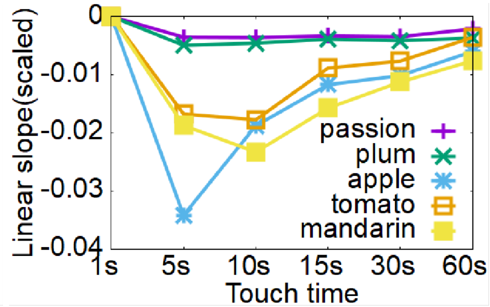

(b) Random touch

Fig. 9. Thermal performance with different touch interaction duration.

Section 6.7, we demonstrate that this is sufficient also for practical scenarios, such as integration with a scale or a self-checkout kiosk.

6.5 Capturing Internal Produce Quality

Tables 4 and 5 illustrate a strong relationship between the linear slope (LS) estimated from thermal dissipation and produce mass (grams) for both long and short interactions, particularly when considering a larger dissipation interval (e.g., 5 seconds in short interactions). Given that mass loss can impact produce quality, as discussed in Section 4.3, these findings demonstrate that SNAKE effectively captures internal produce quality through LS measurements.

Additionally, Figure 7 shows a clear correlation between changes in linear slope over days and variations in produce mass. As produce decomposes and loses mass, the thermal dissipation rate—indicated by the slope magnitude—declines. This decline occurs because key thermal properties, such as thermal conductivity (k), thermal diffusivity (α), and specific heat capacity (C_p), typically decrease during decay.

Figure 10(a) presents the correlation between the average linear slope and thermal properties based on typical values from the literature, as noted in Section 6.1. The linear slope, derived from the total thermal dissipation time in short interactions, consistently shows that weaker thermal properties (lower values) correspond to a lower thermal dissipation rate (smaller slope magnitude), with an average Kendall statistic of $\tau = -0.57$. While some fluctuations exist (e.g., for melon) due to variations in slope during dissipation that a single linear slope cannot fully capture, the slope is generally sufficient for estimating produce quality. Overall, these results indicate that the thermal dissipation rate (or slope) can serve as a reliable indicator of changes in internal produce characteristics and, consequently, produce quality.

We also utilized the target slope in short interactions to predict produce mass. After applying min-max scaling to the mass data, we achieved accurate predictions (RMSE = 0.044, $R^2 = 0.95$) using 5-fold cross-validated regression (Section 6.2) with target slope (TS) and produce type (PU), as shown in Figure 10(b). This performance can be further enhanced by incorporating palm temperature (RMSE = 0.037, $R^2 = 0.97$), as discussed in Section 7. These results reinforce the potential of using thermal dissipation for estimating produce quality.

6.6 Generality and Further Considerations

We next extend the analysis to a wider range of produce types to further demonstrate the generality of our results. We consider 14 produce types (7 types the same as the main study) as depicted in [89], which still covering the main 5 categories of produce: pepo (melon, watermelon, passion fruit), pome (apple, pear), berry (kiwi, tomato,

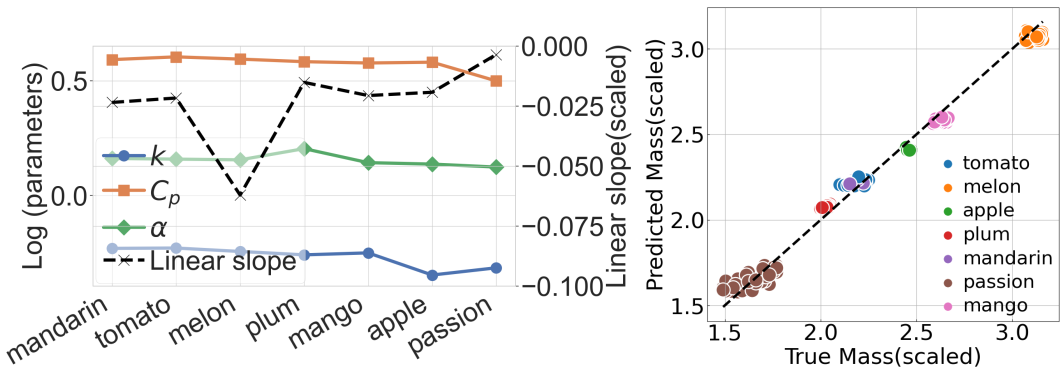

(a) Thermal properties

(b) Performance of mass prediction

Fig. 10. Short interactions: a) Relationship between thermal properties and the linear slope, thermal conductivity k, thermal diffusivity α, and specific heat capacity C_p. b) SNAKE performance, target slope calculated from the first 5 seconds of thermal dissipation.

banana, avocado), drupe (plum, peach, mango) and hesperidium (mandarin, lemon). Pepo and hesperidium fruits generally have a thick epicarp, pomes have a moderately thick epicarp, while berries and most drupes have a thin epicarp. All the new fruits are initially in a fresh and edible state without signs of decomposition. For generality analysis, two samples are still considered for each produce (S1 and S2). Thus, in total 28 fruits are used in the experiment with various shapes and sizes (even the same type). The testbed and measurement remain the same as in Section 5. However, only short interactions (10sec touch) are considered. This study is conducted over a year separate from the main experiment, providing evidence of the generality of SNAKE.

The majority of fruits still exhibited a decrease in firmness over two weeks; however, passion fruit and mandarin follow the main study's trend, and the new lemon aligns with mandarin's pattern. Figure 11 shows the target slope estimated from the first 5 seconds for all fruits in short interactions. We can still observe the distinct slopes of different produce and Kruskal-Wallis tests further verify that the differences are statistically significant (χ^2 = 274.14, η^2 = 0.69, $p < .05$). Besides, Wilcoxon rank-sum tests demonstrate that SNAKE exhibits no significant differences between distinct samples of the same produce ($p > 0.05$). Figure 12 shows a similar target slope trend across all fruits, with Figure 12(a) indicating consistent slopes across different study periods. Statistically, Kolmogorov-Smirnov tests confirm that there is no significant distributional differences in target slopes between the experiment and the main study ($p > 0.05$). This indicates the long-term effectiveness and reliability of SNAKE. Moreover, fruits with hard epicarps, such as pepos, tend to show greater variability in target slope during decomposition than those with thin epicarps, like berries and drupes. Overall, these results strengthen the generalization of SNAKE.

6.7 Other Factors

As the final step, we demonstrate that SNAKE generalizes across different considerations: individuals, storage practices, backgrounds and practical usage. We select a small set of representative produce (mandarin orange, plum, apple, passion fruit, and tomato) from each category to further analyze SNAKE. The testbed follows the design described in Section 5. The interaction time was set to 10 seconds.

Other Users: We recruited 12 participants (6 female and 6 male) to assess the generality of SNAKE across different users. Measurements were collected on 5 different days within a two-week period at days 1, 4, 7, 10

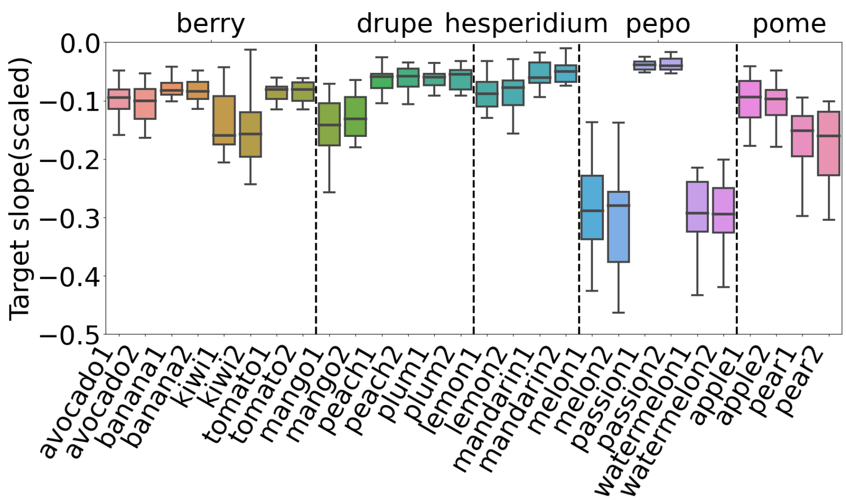

Fig. 11. Target slope of each produce in short interactions

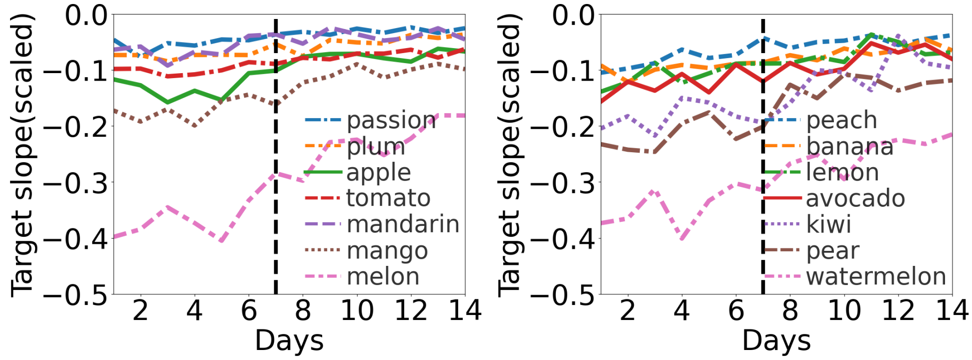

(a) (b)

Fig. 12. Average target slope for all fruits in short interactions

and 14. The average palm temperatures of the participants were 32.01 ± 2.09 °C (male: 32.26 ± 1.96 °C, female: 31.78 ± 2.2 °C). Figure 13(a) shows the target slope (TS) of fruits across all participants over 14 days, and we can observe a similar trend as in our main experiments. This indicates that SNAKE can estimate fruit quality accurately across different users. Figure 13(b) shows the target slope of the plum as an example between male and female participants. We can observe the relative trend is also consistent across genders. A Wilcoxon signed rank test using genders showed no significant differences in the target slope across different days for all the fruits ($p > .05$). Kolmogorov-Smirnov tests further verify that the distribution of target slope is not statistically different ($p > .05$) between the main experiment and our case study (passion fruit: KS=0.4, plum: KS=0.2, apple: KS=0.4, tomato: KS=0.4, mandarin:KS=0.4), see Figure 13(c) with plum as an example. This verifies that the models only depend on produce category and decomposition state, demonstrating the consistency of SNAKE across different individuals.

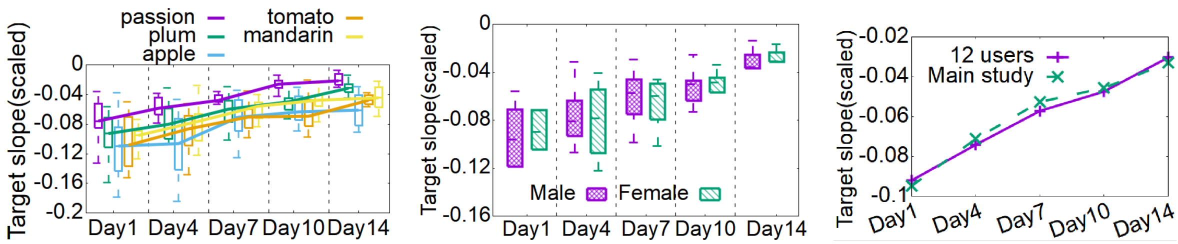

(a) All participants (b) plum (c) plum

Fig. 13. Target slope: a) Different participants; b) Genders; c) The main experiment and user studies.

Storage Practices: The preservation time of fruits can be prolonged by wrapping them inside a protective film or keeping them refrigerated. We next assess how these practices affect SNAKE performance within two weeks. We rely on four new samples (S1, S2, S3 and S4) for each produce (see above) and use them to measure four different experiment conditions considering combinations of protective film (on/off) and storage (refrigerated, 5°C, or ambient room temperature, around 23°C): S1 (5°C+no film), S2(5°C + film), S3 (23°C+film), and S4 (23°C+no film). The relative humidity in the fridge is 48.25 ± 2.49% higher than the room humidity. 5°C is chosen as we observe that some produce types are stored in the cooling system around this temperature from the local supermarkets. Produce in the refrigerator was taken out and held by the hand for 10s at the ambient room temperature. Next, the produce was placed back in the fridge for thermal footprint measurement. The film was removed to take measurements, and then the fruit was wrapped in a new film for each experimental instance.

Figure 14 shows the changes in firmness and target slope for the fruits over the 14 days. The pattern of target slope across days is similar between the fridge and room, although the slope increases slower when the produce is in the fridge. This indicates that SNAKE works well even in very low temperatures. In addition, the results are as expected. Specifically, the protective film and refrigeration slow down decomposition and these effects can be captured using SNAKE. Figure 15(a) further demonstrates less variation in target slope for all fruits (average standard deviation: S1=0.017, S2=0.014, S3=0.022 and S4=0.027) with film and refrigeration, which aligns with the lower variation in firmness changes (average standard deviation: S1=4.10, S2=3.19, S3=5.17 and S4=6.53) shown in Figure 14(a-e). This indicates that SNAKE can perform consistently for produce quality estimation across different conditions. Friedman tests also reveal significant differences in target slope among the four conditions ($\chi^2 = 17.74$, $W = 0.42$, $p < .05$). Even though the apple itself generally has a long shelf life, SNAKE accurately detects subtle variations in target slope under film and refrigeration (standard deviation: S1=0.013, S2=0.011, S3=0.015 and S4=0.018), comparable to the ground-truth firmness (standard deviation: S1=2.8, S2=2.2, S3=3.0 and S4=3.5) shown in Figure 14(c). Indeed, refrigeration results in higher relative humidity than room temperature. The combination of lower temperature and higher relative humidity can minimize moisture loss and preserve produce freshness longer [35]. Wilcoxon Rank-Sum tests also demonstrate the significant differences of storage temperatures ($\chi^2 = 2001$, $p < .05$), indicating better freshness preservation due to refrigeration. In addition, 15(a) reveals a greater median slope amplitude under low temperatures for all produce (refrigerator: average $median = -0.079$, room: average $median = -0.068$). This observation aligns with Newton's Law of Cooling, which states colder environments accelerate thermal dissipation.

Similarly, protective films can enhance produce freshness with larger median slope amplitudes, particularly for thin-skinned fruits, e.g. plum (film = -0.052, no film =-0.043) and tomato (film =-0.052, no film =-0.043) at room temperature. These fruits are highly susceptible to moisture loss due to their permeable skins, which plastic wrap can mitigate. Consequently, plastic wrap is commonly used on cut fruits, as their exposed flesh leads to even faster moisture loss. While mandarin's thick peel offers some protection, it remains vulnerable

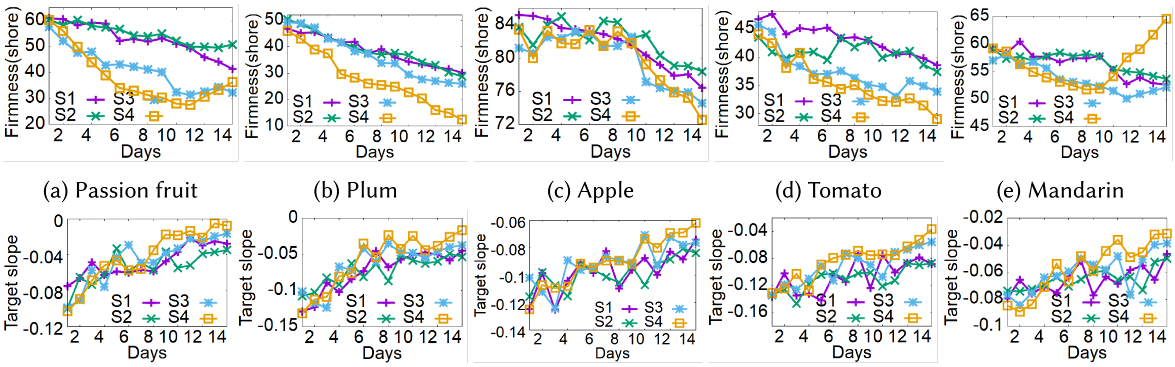

(a) Passion fruit (b) Plum (c) Apple (d) Tomato (e) Mandarin

(f) Passion fruit (g) Plum (h) Apple (i) Tomato (j) Mandarin

Fig. 14. Target slope for different conditions. S: Sample; S1 (5°C+no film), S2(5°C + film), S3 (23°C+film), and S4 (23°C+no film).

to moisture loss and hardening at room temperature due to pores and oil evaporation. Consequently, plastic films significantly slow these processes (film: median = −0.058, no film: median = −0.051), a trend mirrored in firmness changes observed in Figure 14(e). As demonstrated in 15(a), plastic films significantly improve freshness at room or higher temperatures, but their effect is diminished under refrigeration. Nonetheless, the observed results (S1 and S2) still indicate a residual benefit. Therefore, the combination of refrigeration and protective film is the most effective at preserving fruit quality as the variations quantified through the target slope are marginal. The effect of storage practice on SNAKE is evaluated still using the same 5-fold cross-validated regression and classification models as shown in Section 6.2. The input features are target slope (TS), produce type (PU), environment or storage temperature (E) and protective film (F). Results showed that incorporating storage features can incrementally improve average performance: TS+PU (RMSE=0.074, $R^2 = 0.90$, accuracy= 74.7%), TS+PU+E (RMSE=0.065, $R^2 = 0.92$, accuracy=80.4%), TS+PU+E+F (RMSE=0.062, $R^2 = 0.93$, accuracy= 81.2%). Note that the best performance is achieved (RMSE=0.057, $R^2 = 0.95$, accuracy 84.3%) when further adding the palm temperature feature, as depicted in Section 7. These results are in line with current knowledge and highlight how SNAKE generalizes. Furthermore, this result also suggests that SNAKE can be used to analyze the effectiveness of storage strategies.

Effect of background in thermal footage: The amount of thermal radiation that is captured by a thermal camera depends on the *emissivity* (ε) of the background material which corresponds to the fraction of thermal radiation that the material transfers back to the environment. Materials with low emissivity only transfer a small amount of thermal radiation to the environment, but they can reflect heat from objects in their vicinity. Our main study considered a black background which has a high emissivity ($\varepsilon \approx 1$), i.e., it eliminates thermal radiation from the environment. In retail shops the background may vary, resulting in differing emissivity patterns. For example, metal surfaces commonly have low emissivity ($\varepsilon < 0.1$), i.e., they reflect thermal radiation from objects in the environment, whereas high emissivity materials mostly are matte surfaces made of other materials than metals [40, 75], e.g., aluminum foil ($\varepsilon \approx 0.04$), concrete($\varepsilon \approx 0.94$), glass ($\varepsilon \approx 0.94$), wood ($\varepsilon \approx 0.90$), plastic ($\varepsilon \approx 0.96$) and paper ($\varepsilon : 0.91 - 0.95$). Most organic produce also have a high emissivity (>0.95) due to water content of the produce [34, 82]. For example, the emissivity of the apple is in the range $\varepsilon : 0.94 - 0.97$. The emissivity value can usually be specified manually in the camera settings, or the camera can perform periodic self-calibration to estimate the emissivity of the background. To assess the effects of differing backgrounds, Figure 15 (b) compares thermal dissipation times from measurements of 6 participants (5 males and 1 female)

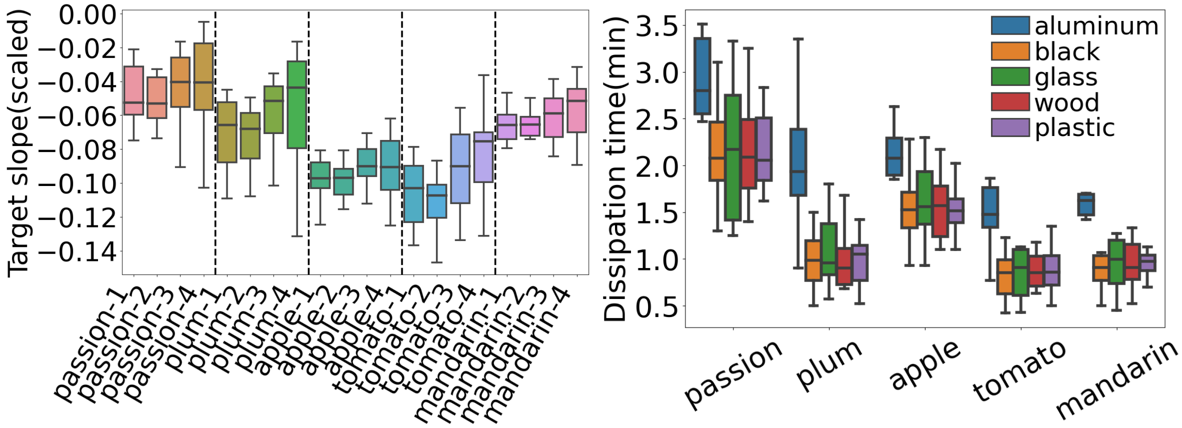

(a) 1-min touch

(b) 10s touch

Fig. 15. a) Target slope for different conditions. 1 (5°C+no film), 2(5°C + film), 3 (23°C+film), and 4 (23°C+no film). b) Thermal dissipation time in different background.

across five different backgrounds (aluminum, black background as in the main study, glass, wood, and plastic). The dissipation patterns are mostly consistent and in line with our experiments, with the only exception being the aluminum background. This indicates that SNAKE can operate robustly against most backgrounds, but highly polished background materials such as aluminum may cause difficulties, and the background should be considered when deploying SNAKE in retail environments.

Practicality: SNAKE has been designed to aid sustainable retail practices for produce during the retail experience. One way to accomplish this in practice is to integrate SNAKE into a product scale or a self-checkout device, as illustrated in Figure 1. To verify the integration would also be feasible in practice, we collected observations from the field by recording the time the consumers used for weighing produce on a scale. The measurements were done using shadowing and carried out in a local supermarket. Generally, when the consumer places the produce on the weight scale, the produce remains still while the user selects the appropriate label from the scale's screen. We used a time application to measure how much time this takes on average, to assess whether there would be sufficient time to estimate the thermal fingerprint of the produce. 50 observations from consumers' weighing times were recorded (male: 23, female: 27). All produce weighing processes were natural without any interference or interruption from the researchers. One outlier (47.95s) was removed for more robust statistical analysis. The average weighing time was 8.55 ± 4.24s, i.e., there would be $4 - 12$ seconds to capture the thermal footprint. As shown by our experiments, this is sufficient for SNAKE to estimate fruit quality.

7 REDUCING PALM TEMPERATURE FLUCTUATIONS

Thermal transfer from the hand to the produce is influenced by the contact between the hand and the produce. When humans touch objects, the touch patterns vary depending on the type of produce and which parts of the hand are in contact with the produce. Additionally, the skin temperature varies between different parts of the hand, with fingers tending to be colder than the palm. These variations can cause fluctuations in thermal transfer and affect the thermal dissipation process. We next illustrate the extent of these variations and introduce a palm compensation model that can be used to mitigate their effects.

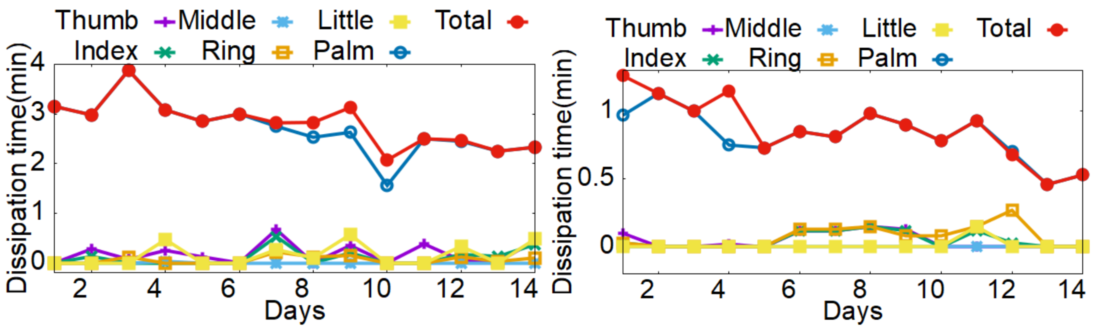

(a) 1-min touch

(b) 10s touch

Fig. 16. Dissipation time of melon in different parts of the hand. Total: thermal fingerprints of the whole hand, i.e., palm and fingers.

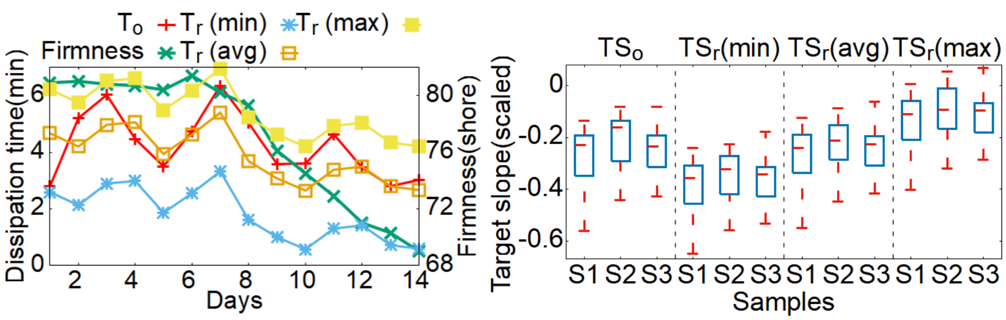

(a) Long interactions: apple

(b) Short interactions: melon

Fig. 17. Temperature compensation (*max*, *min*, *avg*). T_o: original dissipation time, T_r: reference dissipation time, TS_o: original target slope, TS_r: reference target slope.

Thermal Transfer and Touch Patterns: Figure 16 depicts the variation in thermal dissipation times alongside the skin temperature between the palm (32.11 ± 1.40°C) and fingers (31.84 ± 1.47°C). Although the temperature variance between the palm and fingers is minimal, the lower pressure applied by the fingers leads to reduced thermal transfer compared to the palm [83]. Therefore, the part of hand that touches the produce influences thermal dissipation, and ultimately produce quality estimation accuracy, and thermal dissipation should be estimated from contact with the palm whenever possible. This information can be obtained by examining the size of the initial thermal footprint (i.e., the size of the region of interest) or using computer vision.

Quantifying effect of palm temperature: Figure 17 illustrates variations in thermal characteristics as a function of palm temperature. On the left-hand side, we compare how variations in palm temperature affect the estimated thermal dissipation and its relationship to produce firmness using data from a single apple sample collected over a 14-day period. On the right-hand side, we present the target slope estimates for thermal characteristics derived from three different melon samples over the same 14-day measurement period. From the left-hand figure we can observe that temperature fluctuations decrease correlations between produce firmness and thermal dissipation, whereas using a reference model (i.e., the averaged measurements) results in a consistently high correlation between thermal dissipation and produce firmness. The right-hand side figure similarly shows

Table 6. Regression predicting firmness (F) for SNAKE; Features: Thermal dissipation time (T), Target dissipation slope (TS), Palm temperature (P), Produce type (PU).

Sensing modality	Features	Day1/2	Day3/4	Day5/6	Day7/8	Day9/10	Day11/12	Day13/14	5-CV	
		RMSE	RMSE	RMSE	RMSE	RMSE	RMSE	RMSE	RMSE	R^2
Long interactions	**(T,P,PU)**	0.125	0.073	0.058	0.076	0.074	0.098	0.110	0.076	0.935
Short interactions	**(TS,P,PU)**	0.115	0.106	0.076	0.081	0.072	0.079	0.121	0.081	0.925

that slope estimates obtained from individual interactions can fluctuate more than when a reference model (i.e., $TS_r(avg)$ in the figure) is considered. The idea in our compensation model is to reduce these effects by mapping the thermal dissipation measurements to a reference temperature where consistent estimation of thermal dissipation and other thermal characteristics is possible.

Palm compensation model: To address fluctuations in palm temperature, we employ a calibration model that links the estimated thermal dissipation DP_o to a compensated dissipation value DP_r which approximates the thermal dissipation expected at a specified reference palm temperature P_r. Formally, let P_o be the palm temperature of the user; our compensation model approximates the difference in thermal dissipation times between the observed and reference conditions using differences in palm temperature. Specifically, the compensation model for each produce type is defined as $(DP_r - DP_o) = f(P_o - P_r)$ where $(\cdot)$ is the calibration function. We model the relationship using ordinary least squares (OLS) regression and assume the relationship is linear, i.e., $(DP_r - DP_o) = W_p * (P_o - P_r) + C$ where W_p is a weight parameter and C is a constant. For the purposes of this section, we estimate this model from controlled laboratory samples, but in practical deployments, the model can also be learned automatically by using pre-defined palm temperature values as references and comparing thermal dissipation values against this reference. As produce type affects thermal dissipation, we learn the model separately for each type of produce.

Boosting quality estimation: As the final step, we demonstrate that the palm compensation model enhances the performance of SNAKE. We consider the same machine learning models as in Section 6.2. For classification, the accuracy improves by approximately 9% and is consistently high for both long (average: 81.88%: 79.55% RF, 82.66% SVM, and 83.42% MLPC, 82.81%) and short interactions (average: 82.14% RF, 85.45% SVM and 80.86% MLPC). As with our earlier experiments, the differences between short and long interactions are not statistically significant, demonstrating robustness of the compensation values against variations in touch interaction duration. The results for different produce also are similar and produce with harder epicarp tends to have higher performance than other fruits: passion fruit 84.28%, plum 79.29%, apple 80.35%, tomato 82.92%, mandarin 83.02%, mango 85.07% and melon 87.86%.

Figure 18(a-b) shows the confusion matrices for the SVM classifier, which was the best performing classifier in our experiments. From the matrices we can observe that the accuracy is consistently high across the ripeness classes, demonstrating that the palm compensation also improves robustness of SNAKE. The results of regression experiments, summarized in Table 6, similarly show improvements in performance. Both the average RMSE (0.081 for short interactions) and model fit ($R^2 = 0.92$) improve when the palm temperature is utilized. In terms of measurement day, we observe no statistically significant differences across the 14-day period, and we also found no statistically significant differences between the duration of short and long interaction. Finally, in Figure 18(c-d) we can observe that the compensation model improves the correspondence between the firmness of the product and the thermal dissipation time since the measurements closely approximate a linear trend, whereas our earlier results showed that some types of product result in more significant deviations from a linear trend.

In conclusion, when the thermal camera can be used to estimate palm temperature prior to interaction, the accuracy of produce quality estimation provided by SNAKE can be further enhanced by integrating our

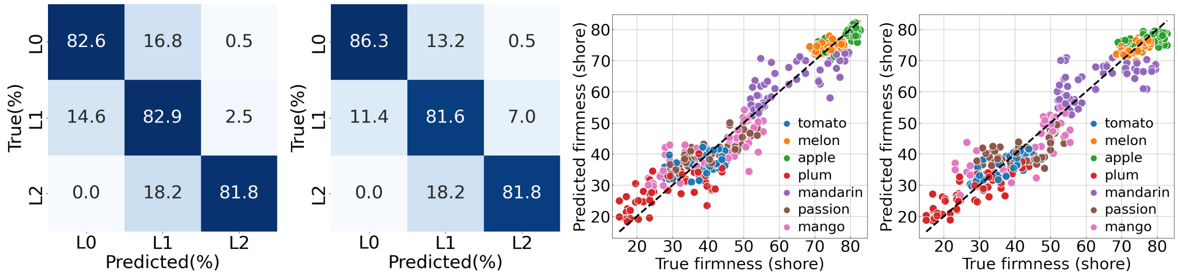

(a) Long interactions(1min) (b) Short interactions(10sec) (c) Long interactions(1min) (d) Short interactions(10sec)

Fig. 18. SNAKE performance boosting by palm temperature, (a)-(b) classification, (c)-(d) regression.

palm compensation model into the system. As the experiments show, the palm compensation model improves consistency across produce types, while at the same time improving estimation accuracy.

8 REDUCING ENVIRONMENT TEMPERATURE FLUCTUATIONS

In a typical retail setting, fresh produce is stored in two primary temperature zones: ambient (room) temperature and refrigerated temperature. The former is maintained by the store's HVAC (heating, ventilation, and air conditioning) system for a stable thermal environment throughout the store. The latter, on the other hand, is regulated by dedicated cooling systems to maintain a consistently lower temperature. Therefore, we can mainly consider two storage temperatures to explore the environmental impact on thermal dissipation. We analyzed SNAKE's performance under refrigerated (5°C) and ambient room temperature (approximately 23°C), as results shown in Section 6.7. Figure 15 (a) demonstrates that SNAKE effectively distinguishes between these conditions, showing larger average slope amplitudes for all produce at lower temperatures. This observation aligns with Newton's Law of Cooling, which states colder environments accelerate thermal dissipation. Thus, from a physics perspective, the target slope TS_o at one temperature E_o (e.g., 5°C) can be adjusted based on the reference slope TS_r at another temperature E_r (e.g., 23°C).

Environmental compensation model: We develop a nonlinear compensation model to account for environmental variations based on the temperature difference E_{diff}: $TS_r = \frac{TS_o - k * E_{diff}}{1 + \beta * E_{diff}}$, where $E_{diff} = E_r - E_o$, and k, β are calibration constants. The numerator offsets the direct effect of temperature shift by subtracting $k * E_{diff}$. However, since linear correction alone may not fully capture the nonlinear behavior of environmental heat exchange, an additional correction factor $(1 + \beta * E_{diff})$ is applied in the denominator to scale the effect of environmental temperature correctly. This term is inspired by Newton's Law of Cooling, which describes how the cooling rate depends on the surrounding environment. Once the compensation equation is applied, we obtain the compensated target slope $TS_o^{'}$. Since our prior results indicate that environmental factors impact the thermal dissipation uniquely for each produce type, we still learn the model separately for each type of produce.

Result: Figure 19 illustrates the environmental temperature compensation for plums and tomatoes as examples, using room temperature (23°C) as the reference. The initial gap between the original TS_o and reference TS_r target slopes highlights the impact of environmental temperature variations. However, after applying the compensation model, the corrected slopes $TS_o^{'}$ closely align with the reference values TS_r, demonstrating that SNAKE maintains consistent performance across different environments. Results in Section 6.7 also show that adding environment temperature (E) feature improves the classification accuracy (80.5%) compared to using only target slope (TS) and produce type (PU) with 74.7% accuracy. In practical applications, the model's coefficients can be fine-tuned to accommodate variations in retail-specific ambient and refrigerated temperatures.

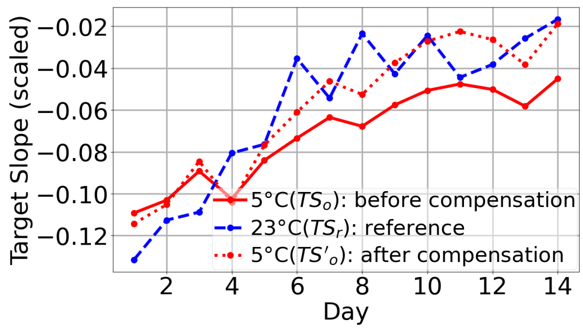

(a) Plum

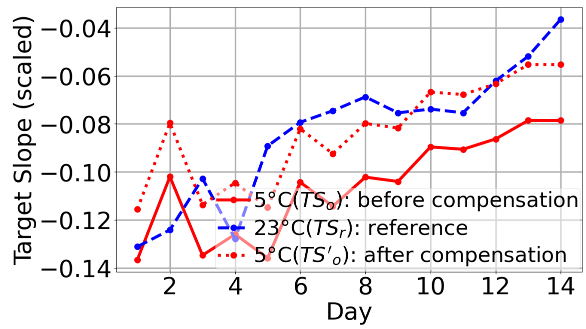

(b) Tomato

Fig. 19. Environmental compensation, TS_o: original target slope, $TS_o^{'}$: compensated target slope, TS_r: reference target slope.

Currently, we use single compensation models to adjust the target slope effectively based on ambient temperature and palm temperature separately, demonstrating that both factors influence produce quality estimation. However, their combined effect requires a more sophisticated model for accurate representation. To accurately capture their interaction on produce quality, we still consider the machine learning models, see Section 6.2. The performance is further improved (RMSE=0.06, R^2 = 0.937, accuracy=82.5%) when considering these four parameters: target slope (T) and produce type (PU), environmental temperature (E) and palm temperature (P). This demonstrates that both ambient and hand temperatures jointly influence the target slope in produce quality assessment.

9 USER STUDY

We finally quantitatively evaluate SNAKE against traditional manual inspections through a comprehensive experiment using short interactions. This study aims to demonstrate how our device can improve consumer purchasing decisions, reduce retail food waste and provide potential economic benefits that justify its adoption in retail.

Application: We developed an Android mobile application on the thermal phone to assess produce quality by analyzing thermal radiation, see Figure 20b. The application is based on the model developed in our main study (short interactions) and we envision integrating the application into the retail weighing scale system. The application workflow involves two steps. When users choose a fruit and place it on the scale, they press "Select a fruit" in the app to capture thermal data and process it. After choosing the produce type (e.g., "apple"), the app classifies its quality into three intuitive levels: Fresh (L0), Not fresh but Edible (L1), and (Near) rotten (L2), helping consumers make informed purchasing decisions. These levels are still coarse-grained to make the content consistent. Note that these labels differ from the technical classification in Section 6.2—Fresh (L0), Active Decay (L1), and Advanced Decay (L2)—but were adapted for better user comprehension while maintaining equivalence in meaning.

Testbed: Figure 20a illustrates our deployment setup, where the thermal phone is integrated into a 3D-printed design that enhances the standard capabilities of a retail-scale appliance [13]. The scale surface is covered with a black background to minimize the influence of ambient environments. This setup emulates real-world purchase scenarios: users select a produce, place it on the scale, and receive a quality assessment via the app (similar to receive a price label). The automated nature of the system reduces the reliance on subjective human judgment

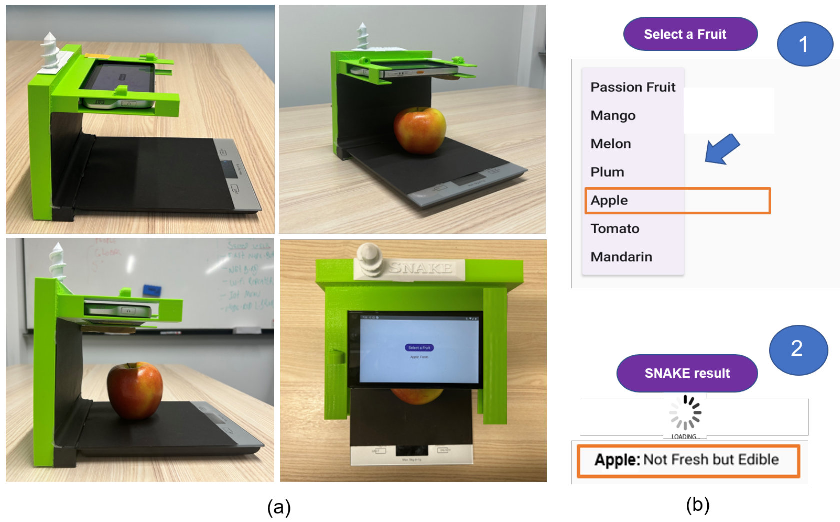

Fig. 20. SNAKE augmenting common scale appliances. a) Integration using a 3D-printed design prototype, b) User interface and application usage.

and helps standardize fruit quality evaluation, which can be beneficial in minimizing food waste and improving overall sales.

Study Design: The study was conducted over two weeks in different areas within the same campus building (see Section 3), where ambient temperature remained consistent with the app model's conditions. We evaluated seven produce types as in Section 5, with two new samples each labeled S1 and S2. Participants were divided into two groups: Group-1 using sample-1 (S1), and Group-2 using sample-2 (S2). Using two samples for each type could reduce the potential for human-induced variations in produce quality, leading to more reliable results than a single sample.

- Group-1 (App-first): Participants first assessed produce quality using the app and then manually inspected the produce with their own habits. In the manual inspection, they were asked to classify each item into one of the three coarse-grained ripeness levels (Fresh, Not Fresh but Edible, (Near) rotten) for comparison.
- Group-2 (Manual-first): Participants performed manual inspection first, followed by app-based evaluation.

After each item evaluation (app/manual), participants were asked: (1) *"Shall we proceed with purchase?"* (YES/NO); and (2) if NO, *"Would you proceed if a discount was offered?"* (YES/NO), with the option to specify a preferred discount if YES. These questions aimed to evaluate how the app influences consumer behavior and purchasing decisions, which are key factors in determining its economic feasibility. The study was conducted over five measurement days (Days 1, 4, 7, 10, and 14), with produce freshly sourced at the start and stored consistently in the same room between survey periods. Each measurement day involved 20 new participants (10 per group), leading to a total of 100 participants (59 males, 41 females, ages 26.75 ± 6.74). Participant data was recorded anonymously. Before the study, participants were briefed on the study goal and app usage. After completing the experiment, they participated in a short interview to assess user perceptions. The post-study questionnaire (below) included five closed-ended questions on a five-point Likert scale—Questions 1-4 (Strongly Agree to Strongly Disagree), while Question 5 (Very Likely to Very Unlikely)—along with an open-ended question for additional feedback. Durometer was still used to capture the ground truth (firmness) over the two weeks.

(1) *Do you agree with this statement "I often buy fruits"?*
(2) *I am familiar with fruit quality testers in supermarkets, like the avocado tester.*
(3) *Would this device enhance your fruit-buying experience?*
(4) *Do you think this device offers valuable insights into the quality and freshness of fruits?*
(5) *Would you use this device if it were available in stores?*
(6) *As mentioned, this device uses heat transferred from your hand to estimate fruit quality. Would you have any concerns about how this data is used?*

Results: We first analyzed the agreement rate between app-based and manual classification to determine how often users aligned with the app's labels. The results showed a higher correspondence in group-1 (74.28%) than in group-2 (49.14%), indicating that the app influences human assessments by at least 25%, with most misalignment occurring between adjacent quality levels in group-1. The agreement rate in group-1 was particularly high for fruits that are difficult to evaluate based on visual appearance, such as apple (82.01%), melon (82.04%), and mango (86.03%), whereas group-2 showed significantly lower agreement for these fruits (apple: 58.01%, melon: 48.04%, mango: 62.03%). This suggests that participants in group-1 relied more on the app, prioritizing internal quality over external appearance, as SNAKE captures internal attributes that may not be visually apparent. However, for fruits that undergo visible decomposition, participants tended to trust their own perceptions over the app's assessment. A key example is passion fruit, which wrinkles easily but remains of good quality. Despite this, many participants still perceived it as inedible even on day-1 of purchase, consistent with the findings discussed in Section 3.1. However, the agreement rate for passion fruit in group-1 (56.05%) was still notably higher than in group-2 (28.05%), highlighting the app's impact on user decision-making in produce quality assessment.

We also assessed the app's impact on purchase decisions by comparing "YES" responses to *"Shall we proceed with purchase?"* across both groups. The app increased the overall purchase rate (73.6%) compared to manual inspection (69.1%), with the most notable increase observed in purchases of "Not Fresh but Edible" produce (app: 60%, manual: 54%), while almost none occurred for "(Near) rotten" produce. Although the app positively impacts sales, the overall increase remains moderate, as its influence on human perception in group-1 results in similar purchase rates for both methods (app: 72%, manual: 71.71%). However, a significant difference is observed in group-2, where the app leads to a higher purchase rate (app: 75.14%, manual: 66.28%), particularly for produce classified as "Not Fresh but Edible", where the app reduces the rejection rate by at least 10% (app: 60.5%, manual: 50.1%). This suggests that the app helps consumers make more informed choices by encouraging the purchase of produce that is still edible while not fresh.

We further analyzed discount acceptance behavior by examining the percentage of initial "NO" responses to purchasing that changed to "YES" when a discount was offered. The results show that more "Not Fresh" fruits were accepted through discounts in both groups, with a higher promotion rate using the app (42.51%) compared to manual inspection (27.69%), indicating a 15% greater acceptance of discounted produce when using the app. This highlights the app's role in reducing food waste by encouraging the purchase of still-edible produce. This trend was consistent across groups (group-1: app 45.5%, manual 30.6%; group-2: app 39.8%, manual 24.7%), suggesting that group differences had little impact. Additionally, discount preferences remained similar across methods, with median values (both methods: 30%) and mean values (app 32% and manual 36%), with participants generally favoring discounts between 15% and 50%. Overall, incorporating the app and discounts increased fruit sales by 88%, compared to 77% using manual inspection and discounts alone. This suggests that SNAKE has the potential to reduce produce waste by at least 10%, with the highest reduction reaching 15% (app: 90%, manual: 74%) in group-2, where user perceptions are less influenced by the app.

Finally, we compared both methods against the ground truth. Overall, SNAKE significantly outperforms manual inspection, achieving an accuracy of 81.4% compared to 61.9% for manual assessment. Performance was consistent across groups (group-1 80.3% and group-2 82.5%), while manual inspection in group-1 (68%) outperforms group-2

(55.7%), suggesting that prior app interaction positively influences users' manual assessment. Note that the app accuracy can be further enhanced by integrating palm temperature measurements, which could be seamlessly automated in retail environments using built-in thermal or temperature sensors. The post-study questionnaire demonstrates that most participants (82%) made independent purchase decisions for reliable assessments. 85% of participants agreed that the device enhances their fruit-buying experience, and 84% found the insights valuable for assessing freshness. Additionally, 92% expressed willingness to use the device in retails, indicating strong potential for adoption. Although only 12% of participants were familiar with existing supermarket fruit testers (e.g., avocado testers), most were open to adopting new technology for produce quality estimation. Importantly, concerns about data usage were minimal, with 90% of respondents stating they had no significant privacy concerns. For example, participant P64 said that *"this technique inspires sustainability and I would love this product"*, and P17 mentioned that *"this technique can help me evaluate the fruits like melon, which cannot be assessed visually"*. However, some concerns remained. P75 mentioned that *"there should be a balance between the data privacy and technology advancements for trustworthiness and transparency"*. P34 worried that *"hand heat data could potentially be misused to infer medical conditions"*, and P62 also said that *"I am concerned about the possibility of fingerprints being captured"*. Overall, these findings highlight SNAKE's practicality and strong consumer acceptance, with the potential to enhance confidence in fruit selection while reducing retail food waste.

10 DISCUSSION

Extensions: The presence of fresh produce on supermarket shelves invites interactions from customers, which can potentially accelerate natural decomposition. Integrating SNAKE can assist retailers in maintaining a desired standard level and mitigate the impact of customer handling produce. Furthermore, the capabilities of SNAKE can be extended to simultaneously evaluate multiple produce at a time, such as those held in both hands. This extension requires employing additional steps in the analysis, e.g., we can identify centroids of the hottest regions from the thermal footage, as done in previous work [12], and apply SNAKE separately on each region. Another potential extension is to extend SNAKE to outdoor scenarios, e.g., outdoor markets or farms. If the outdoor temperature is higher than that of the hands, using touch interactions may no longer be feasible. In this case we can harness sunlight and temporarily block sunlight to estimate dissipation patterns. Our prior work has demonstrated the potential of this strategy for outdoor litter detection [84], and the same principles could be extended to produce.

Produce with small or uneven surfaces: In our main study, SNAKE can assess the quality of passion fruit accurately (e.g., 84.28% in short interactions), even as its surface wrinkles and becomes irregular during ripening with evolving textures. However, certain produce with highly uneven or hazardous surfaces (e.g. pineapple and cactus fruit) may not be suitable for SNAKE. Similarly, smaller organic produce, such as grapes attached to vines, are not suitable for SNAKE as it requires a sufficiently large surface area to obtain a representative sample for quality analysis. Indeed, as our experiments demonstrated, small contact surfaces (such as from the fingers) do not transfer sufficient heat and this also applies to small produce. Besides fruits, fresh produce also includes a large diversity of vegetables. Unlike fruits, vegetables have additional characteristics that require fine-tuning SNAKE before it can be used on them. For instance, vegetable can be leafy, thin and have uneven surfaces. When the produce is placed on an even surface, such as a scale or checkout kiosk, a potential way to overcome this is to induce a thermal signature on the produce, e.g., using an infrared light source and then use SNAKE on this fingerprint.

Other produce and storage practices: Our experiments demonstrated accurate and robust produce quality estimation for the main categories of organic produce. However, in practice the same fruit category can have sub-types that vary from the general pattern (e.g., Fuji and Red Delicious for apples), and thus there may be produce for which the results do not directly translate. This may require constructing separate fingerprints for each produce type to be able to use it accurately. Another important consideration for estimating produce quality is storage practices. Different mechanisms have been developed to extend the shelf life of produce in households, e.g., refrigeration, freezing, and canning. Temperature is a key factor that influences any storage mechanism. Moreover, optimal temperature depends on the type of the produce [11]. For instance, non-chilling sensitive fruits (e.g., apple) can tolerate cooler temperatures and can be stored close to 0°C, while chilling sensitive fruits (e.g., passion fruit) are better stored at a higher temperature (7°C-15°C). Thus, we are also interested in exploring various ambient temperatures to determine the best storage practice for each type [11].

Impact of thermal measurements: The performance of SNAKE depends on the quality of the thermal footage, which can be affected, e.g., by atmospheric transmission and the camera resolution [54, 68]. The atmosphere between the thermal cameras and the object can attenuate infrared radiation emitted by the object and is influenced by the distance between the object and the thermal camera, atmospheric temperature and relative humidity [55, 76]. In practice, when the temperature between the thermal imager and the produce is small ($< \approx$ one meter), atmospheric effects are negligible. At the same time, the maximum distance depends on the camera resolution (our CAT S61: 80 x 60). Our previous research has show 70cm distance between camera and object to be sufficient with this resolution and higher resolutions can support longer distances without it affecting thermal imaging quality.

Emerging applications and practicability: SNAKE targets assisting end-users (retailers and customers) with quality estimation of produce. Thus, any personal device can deploy our method. New wearable devices like a smart ring can be equipped with a thermal sensor that is the least intrusive, more practical and most intuitive to use [87]. A smartphone (with a thermal camera) can also support quality estimation, but it requires first taking a picture. SNAKE could also be used to identify adulteration of produce, which involves improving the appearance of the produce through chemical substances. Beyond consumer use, grocery retailers are increasingly moving to self-service cashiers. SNAKE could be integrated into these devices and adapt pricing based on produce quality.

Implementation Considerations: Integrating thermal sensing technology into retail environments presents challenges related to hardware integration, cost-effectiveness, consumer adoption, and operational efficiency. Deploying thermal cameras or arrays requires an initial investment, with costs ranging from $10 to $500 of each, depending on resolution, and retailers may hesitate without clear financial benefits. Additionally, seamless integration into existing weighing scales and checkout systems is essential to maintain smooth transaction speeds. Consumer concerns about data privacy and the potential complexity of using new technology could also act as barriers to adoption. However, these challenges could be addressed through strategic implementation and automation. For instance, due to their compact size, thermal cameras or arrays can be embedded within existing retail infrastructure (e.g., weighing scales or self-checkout systems) with minimal modifications. Moreover, hand temperature can be opportunistically collected using built-in thermal or temperature sensors, eliminating the need for additional steps from users. The thermal data is processed in real time through retail servers to automate produce quality assessments without slowing down operation efficiency. Results in Section 6.7 show that the 5-second processing time for thermal dissipation aligns with the average weighing duration, which keeps the process smooth. Furthermore, user studies show that SNAKE helps reduce food waste and build customer trust, which contributes potentially to a strong return on investment and long-term benefits for retailers. While consumer adoption is promising, with 92% of participants willing to use the system, privacy concerns can still be mitigated through transparent policies and regulatory compliance. Importantly, only a short touch is needed before measurement, with minimal interaction naturally occurring as the customer selects the fruit. Overall, adoption barriers remain low, making this system practical, scalable, and cost-effective for modern retail.

Other Studies: Given the limited shelf life of produce, our evaluation is based on independent studies conducted over time with the same type items, ensuring the replication and confirmation of our findings. However, while our experiments accounted for a wide range of factors—including different durations, types of produce, touch patterns, and environments—there remains ample opportunity for further research. Our studies aimed to provide various contexts while maintaining a degree of control, which allows for insights into the general applicability of SNAKE. Future research should focus on more uncontrolled studies and extended time spans to encompass a broader array of factors. Retail-specific elements such as store layouts, refrigeration systems, and ventilation, in addition to seasonal variations in ambient temperature and humidity, may significantly affect produce quality over time. Furthermore, handling practices and storage durations could introduce additional variability. Investigating these effects will necessitate longitudinal studies conducted across multiple supermarkets, assessing how environmental fluctuations, seasonal changes, and operational conditions influence the performance of thermal sensing for fruit quality assessment. Understanding these factors could help further refine our method. At the same time, we stress that our results show that SNAKE already offers significant value to both retailers and consumers. This is particularly evident from the user study results, which indicate that SNAKE can enhance purchase intent while also holding the potential to reduce food waste.

Broader Applications: While our work focuses on produce quality estimation using human touch and thermal sensing, the underlying approach has broader applications in food technology and retail. One potential application is in assessing the freshness of other perishable foods, such as bread, dairy, and meat, where human touch can transfer heat and thermal response variations may indicate changes in texture or spoilage levels. In cold storage environments, thermal sensing from human interaction could help detect surface condensation or structural integrity changes in packaged goods. Additionally, thermal-assisted quality assessment could be integrated into self-service kiosks or smart checkout systems, where consumers naturally interact with food items before purchase. This method could enhance food safety monitoring, reduce reliance on subjective visual inspections, and improve consumer confidence in food quality assessments.

11 SUMMARY AND CONCLUSIONS

We contributed SNAKE as an innovative method that harnesses heat transferred from human touch interactions to estimate product quality. The basic principle in SNAKE is to leverage dissipation of thermal radiation transferred from customers to produce to estimate the quality of an item. The main technical challenges are to obtain robust estimates depending on varying interaction patterns with both the size and duration of the interaction causing challenges. SNAKE overcomes variations in touch by integrating computer vision techniques that identify a region interest and focus the estimation on the region with the highest thermal transfer. Variations in touch interaction duration, on the other hand, are overcome by using calibration functions that link interactions with a reference duration and enable robust estimation for other duration values. We also presented an extension of SNAKE that compensates for palm temperature variations for scenarios that can integrate additional techniques for analyzing the palm. Rigorous and extensive evaluations demonstrated that SNAKE achieves accurate and robust performance, reaching up to 83% classification accuracy and low error in regression tasks ($RMSE = 0.081$) when compared to a ground truth obtained from a durometer. We also compared SNAKE with two state-of-the-art baselines, optical sensing and wireless sensing, demonstrating that it consistently outperforms them. We also demonstrate the practicality of SNAKE through a 3D-printed prototype and a user study involving 100 participants. Taken together, our work offers a cost-effective and innovative way to harness everyday human interactions. Specifically, the cost of our solution is $\$10 - \$500$ depending on the resolution of the thermal sensor. SNAKE has also potential to enhance environmental sustainability as it can assist in identifying high quality items without relying on misleading visual assessments, potentially helping to reduce food waste and loss in the long term.

ACKNOWLEDGMENTS

This work was supported by the Estonian Research Council grant (PRG 2725), the European Union and Estonian Research Council via project TEM-TA101, and the Academy of Finland grant 339614. Special thanks to Farooq Dar for discussions around the topic. We would like to thank the reviewers for the anonymous feedback.

REFERENCES

[1] Judith A Abbott. 1999. Quality measurement of fruits and vegetables. *Postharvest biology and technology* 15, 3 (1999), 207–225.
[2] Maimunah Mohd Ali, Norhashila Hashim, Samsuzana Abd Aziz, and Ola Lasekan. 2020. Emerging non-destructive thermal imaging technique coupled with chemometrics on quality and safety inspection in food and agriculture. *Trends in Food Science & Technology* 105 (2020), 176–185.
[3] Hanieh Amani et al. 2020. Current progress in the utilization of smartphone-based imaging for quality assessment of food products: a review. *Critical reviews in food science and nutrition* (2020), 1–13.
[4] Sahar Aseeri, Kyle Condiff, Maximilian Klein, and Baris Unver. 2017. Freedge: Fighting food insecurity with connected infrastructure. In *Proceedings of the 2017 CHI Conference Extended Abstracts on Human Factors in Computing Systems*. 33–38.
[5] Abdelkareem Bedri, Yuchen Liang, Sudershan Boovaraghavan, Geoff Kaufman, and Mayank Goel. 2022. FitNibble: A Field Study to Evaluate the Utility and Usability of Automatic Diet Monitoring in Food Journaling Using an Eyeglasses-based Wearable. In *27th International Conference on Intelligent User Interfaces*. 79–92.
[6] Shimshon Ben-Yehoshua and Victor Rodov. 2002. Transpiration and water stress. In *Postharvest physiology and pathology of vegetables*. CRC Press, 143–197.
[7] Anuja Bhargava and Atul Bansal. 2018. Fruits and vegetables quality evaluation using computer vision: A review. *Journal of King Saud University-Computer and Information Sciences* (2018).
[8] Anuja Bhargava and Atul Bansal. 2021. Fruits and vegetables quality evaluation using computer vision: A review. *Journal of King Saud University-Computer and Information Sciences* 33, 3 (2021), 243–257.
[9] Sourav Bhattacharya, Patrik Floréen, Andreas Forsblom, Samuli Hemminki, Petri Myllymäki, Petteri Nurmi, Teemu Pulkkinen, and Antti Salovaara. 2012. Ma$$iv – An Intelligent Mobile Grocery Assistant. In *2012 Eighth International Conference on Intelligent Environments*. 165–172.
[10] KV Chau, RA Romero, CD Baird, and JJ Gaffney. 1987. Transpiration coefficients of fruits and vegetables in refrigerated storage. *ASHRAE Report 370-RP* (1987).
[11] Alicia Chaves and Noemí Zaritzky. 2018. Cooling and freezing of fruits and fruit products. *Fruit Preservation: Novel and Conventional Technologies* (2018), 127–180.
[12] Farooq Dar, Hilary Emenike, Zhigang Yin, Mohan Liyanage, Rajesh Sharma, Agustin Zuniga, Mohammad A Hoque, Marko Radeta, Petteri Nurmi, and Huber Flores. 2022. The MIDAS touch: Thermal dissipation resulting from everyday interactions as a sensing modality. *Pervasive and Mobile Computing* 84 (2022), 101625.
[13] Farooq Ayoub Dar, Mayowa Olapade, Abdul-rasheed Ottun, Zhigang Yin, Mohan Liyanage, Ulrich Norbisrath, Marko Radeta, Francisco Silva, Xiang Su, Janick Edinger, et al. 2025. TOAD: Profiling and Evaluating 3D Printed IoT Rapid Prototype Designs. *ACM Transactions on Internet of Things* (2025).
[14] Anshuman J Das, Akshat Wahi, Ishan Kothari, and Ramesh Raskar. 2016. Ultra-portable, wireless smartphone spectrometer for rapid, non-destructive testing of fruit ripeness. *Scientific reports* 6, 1 (2016), 1–8.
[15] Valeria De Laurentiis, Sara Corrado, and Serenella Sala. 2018. Quantifying household waste of fresh fruit and vegetables in the EU. *Waste management* 77 (2018), 238–251.
[16] Zhenjiao Du, Xiangquan Zeng, Xiangxin Li, Xiaomeng Ding, Jiankang Cao, and Weibo Jiang. 2020. Recent advances in imaging techniques for bruise detection in fruits and vegetables. *Trends in Food Science & Technology* 99 (2020), 133–141.
[17] Hilary Emenike, Farooq Dar, Mohan Liyanage, Rajesh Sharma, et al. 2021. Characterizing Everyday Objects using Human Touch: Thermal Dissipation as a Sensing Modality. In *2021 IEEE International Conference on Pervasive Computing and Communications (PerCom)*. IEEE, 1–8.
[18] Asle Fagerstrøm, Niklas Eriksson, and Valdimar Sigurdsson. 2020. Investigating the impact of Internet of Things services from a smartphone app on grocery shopping. *Journal of Retailing and Consumer Services* 52 (2020), 101927.
[19] Tarig Faisal, Moath Awawdeh, Daniel Habte, Hala Berhanu, Kibrom Kifle, Lia Misghina, and Anees Bashir. 2021. Smart Cart With Multi-shopping Solutions. *International Journal of Interactive Mobile Technologies* 15, 24 (2021).
[20] Susana C Fonseca, Fernanda AR Oliveira, and Jeffrey K Brecht. 2002. Modelling respiration rate of fresh fruits and vegetables for modified atmosphere packages: a review. *Journal of food engineering* 52, 2 (2002), 99–119.
[21] Ana Lúcia Gabas, Wiclef Dymurgo Marra-Júnior, Javier Telis-Romero, and Vânia Regina Nicoletti Telis. 2005. Changes of density, thermal conductivity, thermal diffusivity, and specific heat of plums during drying. *International Journal of Food Properties* 8, 2 (2005),

233–242.

[22] Eva Ganglbauer, Geraldine Fitzpatrick, and Rob Comber. 2013. Negotiating food waste: Using a practice lens to inform design. *ACM Transactions on Computer-Human Interaction (TOCHI)* 20, 2 (2013), 1–25.

[23] Eva Ganglbauer, Geraldine Fitzpatrick, and Florian Güldenpfennig. 2015. Why and what did we throw out? Probing on reflection through the food waste diary. In *Proceedings of the 33rd Annual ACM Conference on Human Factors in Computing Systems*. 1105–1114.

[24] Mayank Goel et al. 2015. HyperCam: hyperspectral imaging for ubiquitous computing applications. In *Proceedings of the 2015 ACM International Joint Conference on Pervasive and Ubiquitous Computing*. 145–156.

[25] Ella Graham-Rowe, Donna C Jessop, and Paul Sparks. 2014. Identifying motivations and barriers to minimising household food waste. *Resources, conservation and recycling* 84 (2014), 15–23.

[26] Ana Carolina Amaral Gratão et al. 2004. Thermal properties of passion fruit juice as affected by temperature and water content. *Journal of food process engineering* 27, 6 (2004), 413–431.

[27] P Greidanus and MA Verhoeven. 1986. *Product data of tomatoes*. Technical Report. Sprenger Instituut.

[28] Daniel Groeger and Jürgen Steimle. 2018. ObjectSkin: augmenting everyday objects with hydroprinted touch sensors and displays. *Proceedings of the ACM on Interactive, Mobile, Wearable and Ubiquitous Technologies* 1, 4 (2018), 1–23.

[29] Ahmad Anas Nagoor Gunny, Subash CB Gopinath, Asgar Ali, Chalermchai Wongs-Aree, Noor Hasyierah Mohd Salleh, et al. 2024. Challenges of postharvest water loss in fruits: Mechanisms, influencing factors, and effective control strategies–A comprehensive review. *Journal of Agriculture and Food Research* (2024), 101249.

[30] Unsoo Ha, Yunfei Ma, Zexuan Zhong, Tzu-Ming Hsu, and Fadel Adib. 2018. Learning Food Quality and Safety from Wireless Stickers.. In *HotNets*. 106–112.

[31] ASHRAE Handbook and Refrigeration Chapter. 2018. Thermal properties of foods. *ASHRAE Refrigeration Handbook, ASHRAE, Atlanta, GA* (2018).

[32] Mahmood Ul Hasan, Zora Singh, Hafiz Muhammad Shoaib Shah, Jashanpreet Kaur, and Andrew Woodward. 2024. Water loss: A postharvest quality marker in apple storage. *Food and Bioprocess Technology* 17, 8 (2024), 2155–2180.

[33] Shan He, Siying Li, Anindya Nag, Shilun Feng, Tao Han, Subhas Chandra Mukhopadhyay, and Warwick Powel. 2020. A comprehensive review of the use of sensors for food intake detection. *Sensors and Actuators A: Physical* 315 (2020), 112318.

[34] Hans J Hellebrand, Horst Beuche, and Manfred Linke. 2001. Determination of thermal emissivity and surface temperature distribution of horticultural products. In *Sixth international symposium on fruit, nut and vegetable production engineering, Potsdam, Germany*. 1497–1504.

[35] Maarten LATM Hertog, Ruth Ben-Arie, Erika Róth, and Bart M Nicolaı. 2004. Humidity and temperature effects on invasive and non-invasive firmness measures. *Postharvest biology and technology* 33, 1 (2004), 79–91.

[36] Hui Huang, Li Liu, and Michael O Ngadi. 2014. Recent developments in hyperspectral imaging for assessment of food quality and safety. *Sensors* 14, 4 (2014), 7248–7276.

[37] Nazrul Ismail and Owais A Malik. 2022. Real-time visual inspection system for grading fruits using computer vision and deep learning techniques. *Information Processing in Agriculture* 9, 1 (2022), 24–37.

[38] Sara R Jaeger et al. 2018. Buy, eat or discard? A case study with apples to explore fruit quality perception and food waste. *Food Quality and Preference* 69 (2018), 10–20.

[39] Weiwei Jiang et al. 2019. Probing Sucrose Contents in Everyday Drinks Using Miniaturized Near-Infrared Spectroscopy Scanners. *Proceedings of the ACM on Interactive, Mobile, Wearable and Ubiquitous Technologies* 3, 4 (2019), 1–25.

[40] Menglin Jin and Shunlin Liang. 2006. An improved land surface emissivity parameter for land surface models using global remote sensing observations. *Journal of Climate* 19, 12 (2006), 2867–2881.

[41] Isa John et al. 2014. Determination of thermal conductivity and thermal diffusivity of three varieties of melon. *Journal of Emerging Trends in Engineering and Applied Sciences* 5, 2 (2014), 123–128.

[42] Pablo Juliano et al. 2011. The need for thermophysical properties in simulating emerging food processing technologies. *Innovative food technologies: advances in multiphysics simulation. Wiley-blackwell IFT Press, Ames, USA* (2011), 23–38.

[43] Marike Kellermayr-Scheucher, Laura Hörandner, and Patrick Brandtner. 2022. Digitalization at the point-of-sale in grocery retail-state of the art of smart shelf technology and application scenarios. *Procedia Computer Science* 196 (2022), 77–84.

[44] Jyoti A Kodagali and S Balaji. 2012. Computer vision and image analysis based techniques for automatic characterization of fruits-a review. *International Journal of Computer Applications* 50, 6 (2012).

[45] Patrick E Lanigan et al. 2006. Trinetra: Assistive Technologies for Grocery Shopping for the Blind.. In *ISWC*. 147–148.

[46] Chang-Hung Lee, Cheng-Ru Lin, and Ming-Syan Chen. 2005. Sliding window filtering: an efficient method for incremental mining on a time-variant database. *Information systems* 30, 3 (2005), 227–244.

[47] Ruinian Li, Tianyi Song, Nicholas Capurso, Jiguo Yu, Jason Couture, and Xiuzhen Cheng. 2017. IoT applications on secure smart shopping system. *IEEE Internet of Things Journal* 4, 6 (2017), 1945–1954.

[48] Martin Valdemar Anker Lindrup, EunJeong Cheon, Michael B Skov, Dimitrios Raptis, and Rob Comber. 2022. Sustainable Foodtures: Exploring Roles of Future Technology in Sustainable Food Shopping. In *Nordic Human-Computer Interaction Conference*. 1–12.

[49] Yutong Liu et al. 2021. Wi-Fruit: See Through Fruits with Smart Devices. *Proceedings of the ACM on Interactive, Mobile, Wearable and Ubiquitous Technologies* 5, 4 (2021), 1–29.

[50] Markus Löchtefeld, Frederik Møller, Lukas Kyster, Anton Nygaard Petersen, Sture Nicolai Jaqué, Anita Larsen, and Hamzah Ziadeh. 2023. FridgeSort-Improving Fridge Sorting behaviour to reduce Food Waste through a Mobile Serious Game. In *Proceedings of the 22nd International Conference on Mobile and Ubiquitous Multimedia*. 420–427.

[51] Jorge E Lozano. 2009. Thermal properties of foods. *Food Engineering-Volume I* (2009), 70.

[52] Robert Lufu, Alemayehu Ambaw, and Umezuruike Linus Opara. 2020. Water loss of fresh fruit: Influencing pre-harvest, harvest and postharvest factors. *Scientia Horticulturae* 272 (2020), 109519.

[53] Kaveh Malek, Keyvan Malek, and Fahimeh Khanmohammadi. 2021. Response of soil thermal conductivity to various soil properties. *International Communications in Heat and Mass Transfer* 127 (2021), 105516.

[54] Titti Malmivirta, Jonatan Hamberg, Eemil Lagerspetz, Xin Li, Ella Peltonen, Huber Flores, and Petteri Nurmi. 2019. Hot or not? robust and accurate continuous thermal imaging on flir cameras. In *2019 IEEE International Conference on Pervasive Computing and Communications (PerCom*. IEEE, 1–9.

[55] Waldemar Minkina and Daniel Klecha. 2016. Atmospheric transmission coefficient modelling in the infrared for thermovision measurements. *Journal of Sensors and Sensor Systems* 5, 1 (2016), 17–23.

[56] Nuri N Mohsenin. 2020. *Thermal properties of food and agricultural materials*. CRC Press.

[57] Matia Mukama, Alemayehu Ambaw, and Umezuruike Linus Opara. 2020. Thermophysical properties of fruit—a review with reference to postharvest handling. *Journal of Food Measurement and Characterization* 14 (2020), 2917–2937.

[58] Cecilia N Nunes and Jean-Pierre Emond. 2007. Relationship between weight loss and visual quality of fruits and vegetables. In *Proceedings of the Florida State Horticultural Society*, Vol. 120. 235–245.

[59] Robin Nunkoo, Meetali Bhadain, and Shabanaz Baboo. 2021. Household food waste: attitudes, barriers and motivations. *British Food Journal* 123, 6 (2021), 2016–2035.

[60] Mayowa Olapade, Abdul-Rasheed Ottun, Zhigang Yin, Mohan Liyanage, Aleksandr Makarov, and Huber Flores. 2023. Low-cost produce quality monitoring at scale: A practical re-purposing framework for pervasive agriculture. In *Proceedings of the 13th International Conference on the Internet of Things*. 129–137.

[61] AC Paniagua, AR East, JP Hindmarsh, and JAa Heyes. 2013. Moisture loss is the major cause of firmness change during postharvest storage of blueberry. *Postharvest Biology and Technology* 79 (2013), 13–19.

[62] Harold E Pattee. 2012. *Evaluation of quality of fruits and vegetables*. Springer Science & Business Media.

[63] Parisa Pouladzadeh, Shervin Shirmohammadi, and Rana Al-Maghrabi. 2014. Measuring calorie and nutrition from food image. *IEEE Transactions on Instrumentation and Measurement* 63, 8 (2014), 1947–1956.

[64] United Nations Environment Programme. 2024-03. Food Waste Index Report 2024. Think Eat Save: Tracking Progress to Halve Global Food Waste. https://wedocs.unep.org/20.500.11822/45230

[65] Dov Prusky. 2011. Reduction of the incidence of postharvest quality losses, and future prospects. *Food security* 3 (2011), 463–474.

[66] Peter Ragaert, Wim Verbeke, Frank Devlieghere, and Johan Debevere. 2004. Consumer perception and choice of minimally processed vegetables and packaged fruits. *Food quality and preference* 15, 3 (2004), 259–270.

[67] Swati Rallapalli, Aishwarya Ganesan, Krishna Chintalapudi, Venkat N Padmanabhan, and Lili Qiu. 2014. Enabling physical analytics in retail stores using smart glasses. In *Proceedings of the 20th annual international conference on Mobile computing and networking*. 115–126.

[68] Mikko Rinta-Homi et al. 2021. How low can you go? performance trade-offs in low-resolution thermal sensors for occupancy detection: A systematic evaluation. *Proceedings of the ACM on Interactive, Mobile, Wearable and Ubiquitous Technologies* 5, 3 (2021), 1–22.

[69] Alireza Sahami Shirazi et al. 2014. Exploiting thermal reflection for interactive systems. In *Proceedings of the SIGCHI Conference on Human Factors in Computing Systems*. 3483–3492.

[70] Katie Seaborn, Johanna Mähönen, and Yvonne Rogers. 2020. Scaling up to tackle low levels of urban food waste recycling. In *Proceedings of the 2020 ACM Designing Interactive Systems Conference*. 1327–1340.

[71] Mobeen Shahroz, Muhammad Faheem Mushtaq, Maqsood Ahmad, Saleem Ullah, Arif Mehmood, and Gyu Sang Choi. 2020. IoT-based smart shopping cart using radio frequency identification. *IEEE Access* 8 (2020), 68426–68438.

[72] Gözel Shakeri and Claire H McCallum. 2021. Envirofy your shop: Development of a real-time tool to support eco-friendly food purchases online. In *Extended abstracts of the 2021 CHI conference on human factors in computing systems*. 1–10.

[73] Dorian Sinclear, Linda Birch Flensborg, Ask Lindblad Fogsgaard, and Markus Lochtefeld. 2021. Face-the-Waste-Learning about Food Waste through a Serious Game. In *Proceedings of the 20th International Conference on Mobile and Ubiquitous Multimedia*. 67–72.

[74] Vasilis Stavrou and Dimitris Papakyriakopoulos. 2020. Smart Retail: Efficient in-store localization using ensemble classifiers. In *Proceedings of the 24th Pan-Hellenic Conference on Informatics*. 301–304.

[75] F Steiner, F Bleicher, and M Klingenbrunner. 2016. Emissivity Factor of Thermoplastic Materials for a Robot Bending Process. In *Proceedings of the 27th DAAAM International Symposium*. 0664–0670.

[76] Milda Tamošiunaite, Stasys Tamošiunas, Mindaugas Žilinskas, and Milda Tamošiuniene. 2011. Atmospheric attenuation due to humidity. In *Electromagnetic Waves*. IntechOpen.

[77] Sheng Tan, Linghan Zhang, and Jie Yang. 2018. Sensing fruit ripeness using wireless signals. In *2018 27th international conference on computer communication and networks (ICCCN)*. IEEE, 1–9.

[78] R Vadivambal and Digvir S Jayas. 2011. Applications of thermal imaging in agriculture and food industry—a review. *Food and bioprocess technology* 4 (2011), 186–199.

[79] Logan R Vallandingham, Quan Yu, Nakul Sharma, Jo W Strandhagen, and Jan Ola Strandhagen. 2018. Grocery retail supply chain planning and control: Impact of consumer trends and enabling technologies. *IFAC-PapersOnLine* 51, 11 (2018), 612–617.

[80] Hailong Wang, Jiyu Peng, Chuanqi Xie, Yidan Bao, and Yong He. 2015. Fruit quality evaluation using spectroscopy technology: a review. *Sensors* 15, 5 (2015), 11889–11927.

[81] Nan-Nan Wang, Da-Wen Sun, Yi-Chao Yang, Hongbin Pu, and Zhiwei Zhu. 2016. Recent advances in the application of hyperspectral imaging for evaluating fruit quality. *Food analytical methods* 9, 1 (2016), 178–191.

[82] Boran Yang, Govindaraj Dev Kumar, and Kevin Mis Solval. 2022. Evaluation of Low-Cost Smartphone-Based Infrared Cameras to Assess the Cooling and Refrigerated Storage Temperatures of Fresh Produce. *Foods* 11, 21 (2022), 3440.

[83] Zhigang Yin, Mohan Liyanage, Abdul-Rasheed Ottun, Souvik Paul, Agustin Zuniga, Petteri Nurmi, and Huber Flores. 2023. HIPPO: Pervasive Hand-Grip Estimation from Everyday Interactions. *Proceedings of the ACM on Interactive, Mobile, Wearable and Ubiquitous Technologies* 6, 4 (2023), 1–30.

[84] Zhigang Yin, Mayowa Olapade, Mohan Liyanage, Farooq Dar, Agustin Zuniga, Naser Hossein Motlagh, Xiang Su, Sasu Tarkoma, Pan Hui, Petteri Nurmi, et al. 2022. Toward city-scale litter monitoring using autonomous ground vehicles. *IEEE Pervasive Computing* 21, 3 (2022), 74–83.

[85] Xinyang Yu et al. 2016. Development of a handheld spectrometer based on a linear variable filter and a complementary metal-oxide-semiconductor detector for measuring the internal quality of fruit. *Journal of Near Infrared Spectroscopy* 24, 1 (2016), 69–76.

[86] Yue Yu, Sophia Yi, Xi Nan, Leo Yu-Ho Lo, Kento Shigyo, Liwenhan Xie, Jeffry Wicaksana, Kwang-Ting Cheng, and Huamin Qu. 2023. FoodWise: Food Waste Reduction and Behavior Change on Campus with Data Visualization and Gamification. In *Proceedings of the 6th ACM SIGCAS/SIGCHI Conference on Computing and Sustainable Societies*. 76–83.

[87] Tengxiang Zhang et al. 2020. Thermalring: Gesture and tag inputs enabled by a thermal imaging smart ring. In *Proceedings of the 2020 CHI Conference on Human Factors in Computing Systems*. 1–13.

[88] Liyong Zhou, Vikram Chalana, and Yongmin Kim. 1998. PC-based machine vision system for real-time computer-aided potato inspection. *International journal of imaging systems and technology* 9, 6 (1998), 423–433.

[89] Agustin Zuniga, Huber Flores, and Petteri Nurmi. 2021. Ripe or Rotten? Low-Cost Produce Quality Estimation Using Reflective Green Light Sensing. *IEEE Pervasive Computing* 20, 3 (2021), 60–67.